Natural and Industrial Analogues for Release of CO_2 from Storage Reservoirs: Identification of Features, Events, and Processes and Lessons Learned

Jennifer L. Lewicki

Jens Birkholzer

Chin-Fu Tsang

Earth Sciences Division

Earnest Orlando Lawrence Berkeley National Laboratory

Berkeley, California 94720

February 2006

This work was supported by the U.S. Environmental Protection Agency, Office of Water and Office of Air and Radiation for funding this study under an Interagency Agreement with the U.S. Department of Energy at the Lawrence Berkeley National Laboratory, contract number DE-AC02-05CH11231. We thank J. Apps and A. Cortis for constructive review of this report.

EXECUTIVE SUMMARY

The injection and storage of anthropogenic CO_2 in deep geologic formations is a potentially feasible strategy to reduce CO_2 emissions and atmospheric concentrations. While the purpose of geologic carbon storage is to trap CO_2 underground, CO_2 could migrate away from the storage site into the shallow subsurface and atmosphere if permeable pathways such as well bores or faults are present. Large-magnitude releases of CO_2 have occurred naturally from geologic reservoirs in numerous volcanic, geothermal, and sedimentary basin settings. Carbon dioxide and natural gas have also been released from geologic CO_2 reservoirs and natural gas storage facilities, respectively, due to influences such as well defects and injection/withdrawal processes. These systems serve as natural and industrial analogues for the potential release of CO_2 from geologic storage reservoirs and provide important information about the key features, events, and processes (FEPs) that are associated with releases, as well as the health, safety, and environmental consequences of releases and mitigation efforts that can be applied.

We describe a range of natural releases of CO_2 and industrial releases of CO_2 and natural gas in the context of these characteristics. Based on this analysis, several key conclusions can be drawn, and lessons can be learned for geologic carbon storage. First, CO_2 can both accumulate beneath, and be released from, primary and secondary reservoirs with capping units located at a wide range of depths. Both primary and secondary reservoir entrapments for CO_2 should therefore be well characterized at storage sites. Second, many natural releases of CO_2 have been correlated with a specific event that triggered the release, such as magmatic fluid intrusion or seismic activity. The potential for processes that could cause geomechanical damage to sealing cap rocks and trigger the release of CO_2 from a storage reservoir should be evaluated. Third, unsealed fault and fracture zones may act as fast and direct conduits for CO_2 flow from depth to the surface. Risk assessment should therefore emphasize determining the potential for and nature of CO_2 migration along these structures. Fourth, wells that are structurally unsound have the potential to rapidly release large quantities of CO_2 to the atmosphere. Risk assessment should therefore be focused on the potential for both active and abandoned wells at storage sites to transport CO_2 to the surface, particularly at sites with depleted oil or gas reservoirs where wells are abundant. Fifth, the style of CO_2 release at the surface varies widely between and within different leakage sites. In rare circumstances, the release of CO_2 can be a self-enhancing and/or eruptive process; this possibility should be assessed in the case of CO_2 leakage from storage reservoirs. Sixth, the hazard to human health has been small in most cases of large surface releases of CO_2. This could be due to implementation of public education and CO_2 monitoring programs; these programs should therefore be employed to minimize potential health, safety, and environmental effects associated with CO_2 leakage. Finally, while changes in groundwater chemistry were related to CO_2 leakage due to acidification and interaction with host rocks along flow paths, waters remained potable in most cases. Groundwaters should be monitored for changes that may be associated with storage reservoir leakage.

Table of Contents

Figures

Tables

1 INTRODUCTION

The injection and storage of anthropogenic CO_2 in deep geologic formations is a potentially feasible strategy to reduce CO_2 emissions and atmospheric concentrations [e.g., International Energy Agency, 1997; Reichle et al., 1999]. While the purpose of geologic carbon storage is to trap CO_2 underground, CO_2 could migrate away from the storage site into the shallow subsurface and atmosphere if permeable pathways such as well bores or faults are present. Although limited CO_2 leakage does not negate the net reduction of CO_2 emissions to the atmosphere, adverse health, safety, and environmental risks associated with elevated CO_2 concentrations must be evaluated, particularly if the release at the surface occurs quickly and/or is spatially focused. Large-magnitude releases of gas (e.g., CO_2, natural gas) from depth to the near-surface environment that have occurred in natural and industrial settings can serve as analogues for the potential release of CO_2 from geologic storage sites [e.g., Allis et al., 2001; Stevens et al., 2001a; Stevens et al., 2001b; Benson et al., 2002; Beaubien et al., 2004; Shipton et al., 2004; NASCENT, 2005]. Analysis of these analogues thus provides important insight into the key characteristics of the CO_2 release, the resulting impacts of the release on human health and safety, ecology, and groundwater the effectiveness of remedial measures applied. Lessons can then be learned from natural and industrial analogues for risk assessment associated with geologic injection and storage.

The features, events, and processes (FEPs) relevant to the geologic disposal of radioactive waste have been compiled and used in systems analysis to assess the performance and safety of this disposal [e.g., NEA/OECD, 2000]. Based on this work, Savage et al. [2004] developed a framework for compiling a database of generic FEPs for the evaluation of CO_2 storage sites. However, FEPs associated with geologic sequestration of CO_2, in particular potential CO_2 leakage from storage sites, have not been identified from actual cases of leakage from natural reservoirs. The purpose of this report is to discuss the causes and consequences of large releases of CO_2 related to natural and industrial processes, placing emphasis on the geologic model for CO_2 accumulation in the reservoir, events leading to the release of the CO_2 from the reservoir, pathways for CO_2 migration to the surface, the magnitude and consequences of the release, and remedial strategies applied. To this end, we first summarize, compare, and contrast the FEPs of a comprehensive (although not exhaustive) set of natural and industrial large releases of CO_2 (Section 2.1). Second, we describe natural analogues for large release of CO_2 in volcanic-magmatic, geothermal, and sedimentary basin systems, discussing releases of CO_2 from two volcanic-magmatic systems (Mammoth Mountain, California and Solfatara, Italy) in detail (Section 2.2). Third, we describe large releases of CO_2 and natural gas associated with industrial processes (Section 2.3). Fourth, we briefly present the consequences of natural CO_2 releases for groundwater quality (Section 3). We then summarize the primary causes and consequences of large CO_2 releases from natural and industrial settings, and discuss implications for geologic carbon sequestration and related risk assessment work (Section 4).

2 LARGE-MAGNITUDE RELEASES OF CO_2

2.1. FEATURES, EVENTS AND PROCESSES (FEPS)

2.1.1. Overview of natural and industrial analogues

In order to compare and contrast the key characteristics of large natural and industrial releases of CO_2, we classified a range of CO_2 releases according to the key features of the CO_2 accumulation, the events leading to the release of CO_2, and the processes by which the CO_2 was released at the surface (Tables 2.1 and 2.2). In Tables 2.1 and 2.2, columns one through three describe the key features, including site location, the source of the CO_2 in the natural accumulation, and the geologic model for CO_2 accumulation, for example, the reservoir, reservoir depth (if known), and capping rocks. Column four in Tables 2.1 and 2.2 describes the event triggering the release of CO_2 from the reservoir. Columns five and six give the processes by which the CO_2 was released at the surface, including the pathway(s) for leakage and the type of surface release. Table A.1 (Appendix) additionally summarizes for each site the geographic setting and land use, the magnitude and consequences of the CO_2 release, and the remedial measures taken. References for each of the analogues are found in Sections 2.2 and 2.3.

Table 2.1. Summary of natural (N) large releases of CO_2. See Section 2.2 for references.

Site	CO_2 Source	Geologic model for accumulation	Event triggering leakage	Pathway for leakage	Type of release
N.1. Mammoth Mountain, CA USA	Magmatic + thermal decomposition of carbonates	Accumulation at ~2 km depth in porous/fractured rock under caprock	Seismic activity and reservoir pressurization	Faults and fractures	Fast, diffuse, vent, spring
N.2. Solfatara, Italy	Magmatic + thermal decomposition of carbonates	Relatively shallow zone of fractured rock contains gas phase and overlies aquifers, then magma body at several km depth	Not indentified	Faults and fractures	Diffuse and vent
N.3. Mátraderecske, Hungary	Geothermal/copper -zinc mineralization	CO_2 accumulates in karst water reservoir (~1 km depth)	Not indentified	Faults and fractures	Diffuse, vent, spring
N.4. Latera caldera, Italy	Thermal decomposition of carbonates, magmatic component	CO_2 accumulates in liquid-dominated, carbonate geothermal reservoir capped by hydrothermally altered volcanics	Not indentified	Faults and fractures	Diffuse, vent, spring
N.5. Albani Hills, Italy	Magmatic + thermal decomposition of carbonates	Deep pressurized reservoirs in structural highs of sedimentary bedrock	Slow releases with several sudden large releases also occurring, possibly triggered by seismic activity	Faults and fractures	1995 and 1999 events Fast, diffuse, vent, spring/well
N.6. Dieng, Indonesia	Magmatic	Unknown	Volcanic, possibly “pneumatic”, eruptions	Fissure	Eruptive
N.7. Rabaul, Papua New Guinea	Magmatic	Unknown	Unknown	Fractures	Fast, vent
N.8. Lakes Monoun and Nyos, Camaroon	Magmatic	Accumulation in deep lake and stable stratification	Rapid lake turnover triggered at Monoun by landslide; Nyos trigger unknown	NA	Eruptive (limnic)
N.9. Laacher See, Germany	Magmatic	NA	Seasonal lake overturn and mixing	NA	Diffusive and bubbling from lake surface, diffuse from lake shore

Site	CO_2 Source	Geologic model for accumulation	Event triggering leakage	Pathway for leakage	Type of release
N.10. Clear Lake, CA, USA	Thermal decomposition of metasedimentary rocks, minor magmatic component	CO_2 derived from liquid-dominated geothermal reservoir hosted in marine metasedimentary rocks	Not indentified	Faults and fractures	Gas vents, springs
N.11. Paradox Basin, UT, USA	Thermal decomposition of carbonates	Reservoirs are vertically stacked, sandstone units, in fault-bounded anticlinal folds, capped by shale/siltstone units	Not indentified	Faults and fractures	Diffuse, gas seeps, springs
N.12. Florina Basin, Greece	Thermal decomposition of carbonates	Reservoirs are vertically stacked, limestone and sandstone units (upper unit at 300 m depth), capped by silts and clays.	Not indentified	Slow leakage along rock discontinuitie s	Springs, gas seeps

Table 2.2. Summary of industrial (I) large releases of CO_2. See Section 2.3 for references.

Site	CO_2 Source	Geologic model for accumulation	Event triggering leakage	Pathway for leakage	Type of release
I.1. Sheep Mountain, CO, USA	Thermal decomposition of carbonates	Reservoir is anticlinal fold, bounded on one side by thrust fault, sandstone, ave. depth 1500 m, capped by marine sediments and a laccolith.	Well blowout	Well	Free flowing CO_2 gas from well, CO_2 leakage from fractures above drill site
I.2. Crystal and Tenmile Geysers, Paradox Basin, UT, USA	Thermal decomposition of carbonates	Reservoirs are vertically stacked, sandstone units, in fault-bounded anticlinal folds, capped by shale/siltstone units	Well blowouts	Wells	Cold geysers
I.3. Florina Basin, Greece	Thermal decomposition of carbonates	Reservoirs are vertically stacked, limestone and sandstone units (upper unit at 300 m depth), capped by silts and clays.	Well blowout	Well	CO_2 gas leakage from soils, water-filled pool formation around well
I.4. Torre Alfina geothermal field, Italy	Geothermal	Geothermal reservoir with a gas CO_2 cap at ~660 m depth, capped by sequences of shales, marls, and limestones.	Well blowout	Well	Free flowing CO_2 gas from well, diffuse emissions from ground around well

2.1.2. Common and Unique FEPs

Tables 2.1 and 2.2 show that there are several key similarities between the FEPs associated with different CO_2 releases. First, the sources of CO_2 in natural accumulations are most commonly thermal decomposition of carbonate-rich sedimentary rocks and/or degassing of magma bodies at depth (analogues N1, N2, N4-N12, I1-I4). Second, CO_2 from these sources often accumulates in highly fractured and/or porous rocks (e.g., sandstones, limestones) under low-permeability cap rocks (analogues N1-N5, N10-N12, I1-I4). The cap rocks may be low-permeability rock units (e.g., shale, siltstone) or a zone of hydrothermal alteration. In the case of natural CO_2 releases,

once the CO_2 leaks from the storage reservoir, fault and/or fracture zones are the primary pathways for CO_2 migration to the surface. In the case of natural CO_2 leakage, once the CO_2 leaks from the storage reservoir, fault and/or fracture zones are the primary pathways for CO_2 migration to the surface (analogues N1-N7, N10-N12). These high-permeability zones may be pre-existing, or be created/enhanced due to seismic activity associated with, e.g., fluid migration and pore-fluid pressurization. In the case of CO_2 leakage associated with industrial activity, the event triggering the release is commonly a well blowout, related to injection/withdrawal practices or a defect in a well (analogues IB1-I4). Also, the pathway for CO_2 migration to the surface is usually the well bore and/or fractures that have formed around the well bore.

There are several key differences between the FEPs of the various examples of CO_2 leakage (Tables 2.1 and 2.2). The depth of the source of the CO_2 and the reservoir(s) in which the CO_2 accumulates varies widely from < 1 km (e.g., analogues I3, I4) to multiple km (e.g., analogues N1, I1). At an individual site, CO_2 may accumulate in a single reservoir (e.g., analogues N1, N3, N4, N10, I4), or within multiple vertically stacked and/or horizontally compartmentalized reservoirs (analogues N11, N12, I2, I3). Cap rocks and/or low-permeability fault zones can serve to separate multiple CO_2 reservoirs at a given site.

Some examples of natural CO_2 leakage have been correlated with specific triggering events, such as seismic activity or magmatic fluid injection (analogues N1, N5, N6, N8, N9), while other events have not been correlated with such events. However, the lack of correlation in the latter cases may be due to the absence of observations or data collection at the time of the leakage event. Where a trigger event was identified, it was commonly an event that caused geomechanical damage to cap rocks sealing the CO_2 reservoir.

Finally, the style of natural CO_2 leakage at the surface varies widely between different sites, as well as within individual sites. Surface releases occur in the form of diffuse gas emission over large land areas, focused vent emissions, eruptive emissions, degassing through surface water bodies, and/or release with spring discharge (analogues N1- N5, N7, N9, N10-N12). In rare cases, the CO_2 release may have been a self-enhancing or eruptive process (analogues N6, N8). In the case of CO_2 leakage associated with well failures, CO_2 may be emitted at the surface in a focused form as free flowing or geysering CO_2 from the well and/or diffusely through soils, water pools, or fractures around the well site (analogues I1-I4).

2.1.3. Lessons Learned

Several lessons can be learned from both natural and industrial large releases of CO_2 and applied to risk assessment associated with geologic carbon sequestration. First, CO_2 can both accumulate beneath, and be released from, primary and secondary reservoirs with capping units located at a wide range of depths. Both primary and secondary reservoir entrapments for CO_2 should therefore be well characterized at storage sites. Second, the potential for processes that could cause geomechanical damage, such as seismic activity, and trigger the release of CO_2 from a storage reservoir should be carefully evaluated. Next, since unsealed fault and fracture zones act as fast and direct flow paths for CO_2 from depth to the surface, risk assessment should be focused on determining the potential for and nature of CO_2 migration along these structures. Also, wells that are either initially structurally unsound, or become so through injection processes, have the potential to rapidly release large quantities of CO_2 to the atmosphere. Risk

assessment should therefore be focused on injection, withdrawal, and abandoned wells at storage sites, particularly at sites with depleted oil or gas reservoirs where wells are abundant. Finally, in rare circumstances, the release of CO_2 can be a self-enhancing and/or eruptive process; this possibility should be assessed in the case of CO_2 leakage from storage reservoirs.

2.2. NATURAL ANALOGUES

2.2.1. Introduction

Large-magnitude releases of CO_2 have occurred naturally from geologic reservoirs in numerous volcanic, geothermal, and sedimentary basin settings. These systems serve as natural analogues for the potential release of CO_2 from storage reservoirs and provide important information about the key features, events, and processes that are associated with releases, as well as the health, safety, and environmental consequences of releases and mitigation efforts. Here, we begin with detailed descriptions of these aspects of large CO_2 releases at Mammoth Mountain (USA) and Solfatara volcano (Italy); due to the large number of geologic, geophysical, geochemical, and CO_2 degassing data available for these sites. We then follow with more limited descriptions of CO_2 releases in other volcanic, geothermal, and sedimentary basin systems. Each of these releases is summarized with respect to their key characteristics and remedial measures applied in Appendix A (Table A1). While we do not describe all natural large releases of CO_2 that have occurred worldwide, we address a suite of large releases that have been well documented in the literature and represent a range of geologic settings.

2.2.2. Mammoth Mountain, California, USA

Geologic background. Mammoth Mountain (3368 m) is a seismically active, dacitic cumulovolcano located on the southwestern rim of Long Valley caldera (LVC), eastern California (Figure 2.1). The regional geology has been described in detail by Bailey [1989]. LVC lies in a left-stepping offset along the eastern escarpment of the Sierra Nevada at the northern end of the Owens Valley and the western margin of the Basin and Range province. This is an area of closely coupled tectonism and magmatism characterized by crustal extension, basaltic underplating, and crustal intrusion. LVC formed 760,000 years ago by the eruption of 600 km^3 of solid rock equivalent, creating a 32 x 17 km caldera [Bailey et al., 1976; Hill et al., 1985; Bailey, 1989]. A resurgent dome subsequently formed within LVC and is now 10 km in diameter and 500 m above surrounding moat. The Bishop tuff, the product of caldera-forming eruptions, in the LVC moat is underlain by bedrock composed of meta-volcanics and meta-sedimentary rocks corresponding to the Sierra Nevada roof pendants.

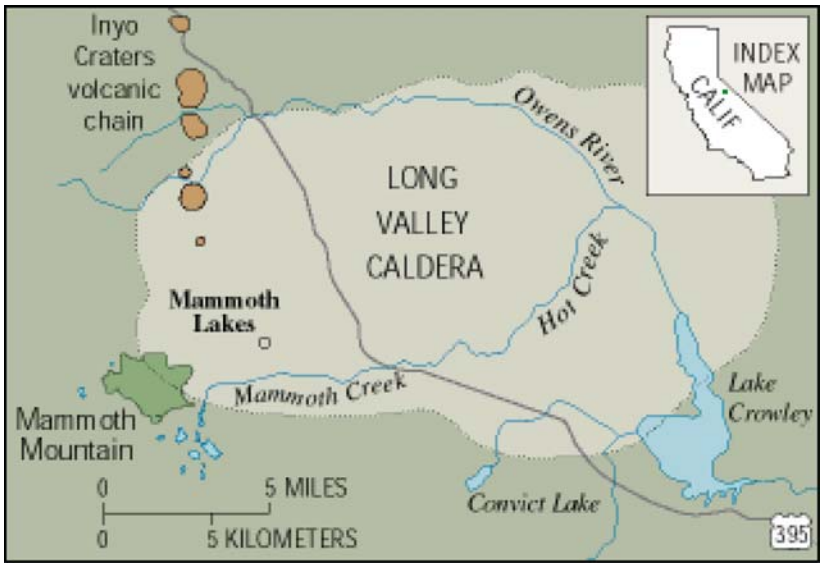

Figure 2.1. Map showing location of Mammoth Mountain on eastern rim of Long Valley caldera, eastern California [http://pubs.usgs.gov/fs/fs172-96/].

The Mono-Inyo Craters volcanic chain is the most recently active system associated with LVC and is localized along a north-trending fissure system extending from south of Mammoth Mountain through the western moat of LVC to the north shore of Mono Lake. This system first erupted basalt and andesite in the west moat of LVC 400,000 to 60,000 years ago and then in the Mono Basin 40,000 to 13,000 years ago [Miller, 1985; Bailey, 1989]. Mammoth Mountain was formed 110,000 to 57,000 years ago by repeated eruptions of dacite and rhyodacite domes and lava flows from vents on the southwest rim of LVC lying within a field of 160-8 ka mafic vents. Magma is thought to be deeper than 3 to 4 km beneath the resurgent dome, while the Mono-Inyo Craters volcanic chain is underlain by a shallower dike-like feeder system [e.g., Fink, 1985; Miller, 1985]. While contiguous, the magmatic system of Mammoth Mountain is distinct from those of LVC and the Mono craters [Hildreth, 2004]. Mammoth is bordered on the west and south by granitic rocks of the Sierran block. Volcanics, meta-volcanics, and meta-sediments crop out in the area surrounding Mammoth. The deep reservoir and up-flow zone of the hydrothermal system in the caldera are hosted in meta-sedimentary basement beneath the West Moat [Sorey et al., 1991].

Hydrology. Mammoth Mountain receives heavy snowfall. The ground surface here, composed mainly of pumice, glacial till, volcanic and granitic rocks, is highly permeable to infiltration, resulting in little direct runoff [Evans et al., 2002]. The volcano edifice is characterized by low temperatures and limited ground water flow, except in shallow outflow zones, and lacks a shallow hydrothermal reservoir. Ground water outflow is focused by lava flows or other laterally extensive units into high-discharge springs on the lower flanks of the volcano [Evans et al., 2002].

Recent activity. Recent unrest associated with Mammoth Mountain was first detected in late 1979 and has been characterized since by ground deformation, swarms of small earthquakes ($M \leq 3$), rapid fire bursts of small earthquakes (spasmodic bursts), long-period (LP) and very long-period (VLP) earthquakes (see Chouet [1996] for definitions), elevated $^{3}He/^{4}He$ ratios in

fumarolic gases, and diffuse CO_2 emissions resulting in large areas of tree kill. Figure 2.2 summarizes the time history of these events and Hill and Prejean [2005] describe these aspects of recent volcanic unrest at Mammoth Mountain in detail.

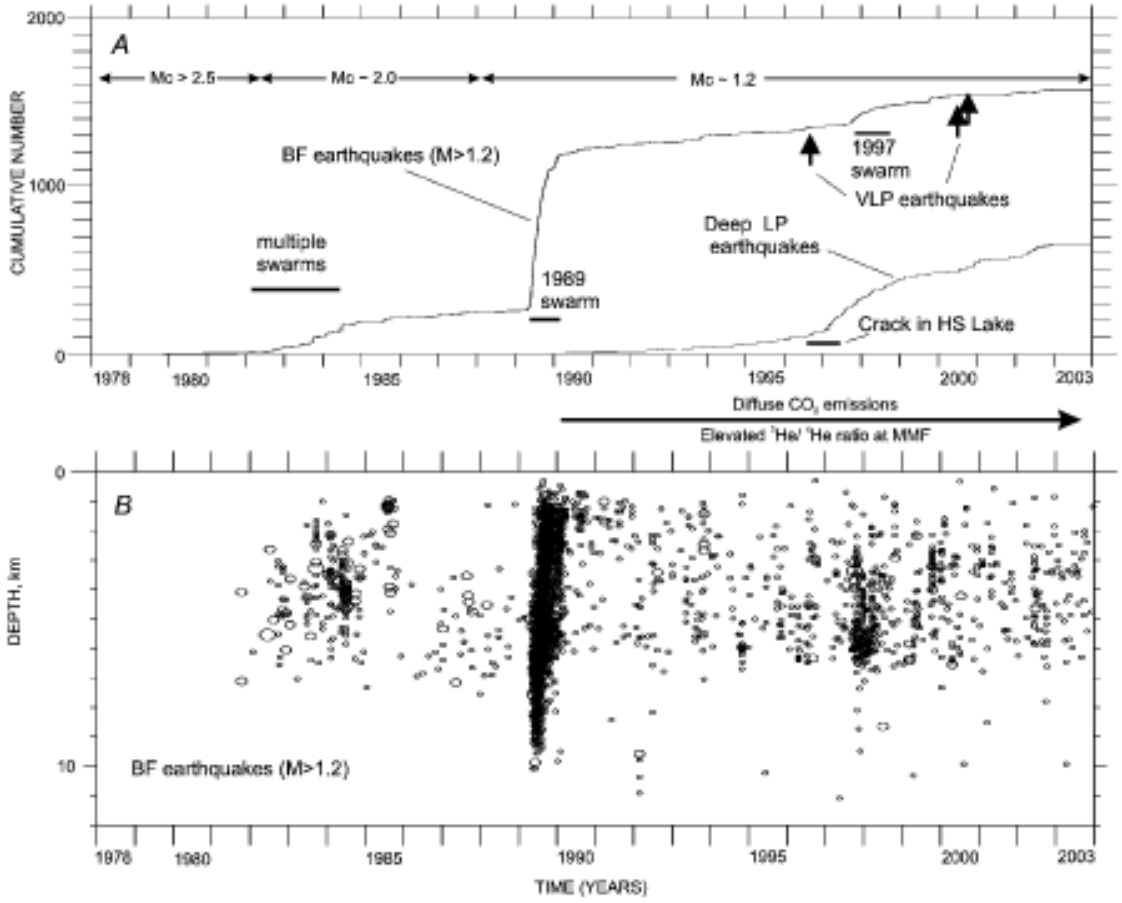

Figure 2.2. (A) Cumulative number of M≥1.2 brittle failure (BF) and long-period (LP) earthquakes versus time at Mammoth Mountain (from Hill and Prejean [2005]). Also shown is the timing of earthquake swarms, diffuse CO_2 degassing, elevated $^3He/^4He$ ratios at Mammoth Mountain fumarole, the formation of a crack in the bottom of Horseshoe (HS) Lake, and very long period (VLP) earthquakes. (B) BF focal depths versus time. Circle size is proportional to magnitude in three steps: 1.2≤M≤1.9, 2.0≤M≤2.9, and 3.0≤M≤3.9.

A notable eleven-month-long seismic swarm occurred beneath Mammoth Mountain, beginning in May 1989 [Hill et al., 1990]. The swarm included >3000 earthquakes of M>0, including three M>3 earthquakes. The cumulative seismic moment for the duration of the seismic swarm was the approximate equivalent of a single M~4.0 earthquake, and the swarm had a high *b*-value, where *b* is the coefficient of the frequency-magnitude relation ($\log N = a - bM$). Prejean et al. [2003] used the double-difference earthquake location algorithm [Walhauser and Ellsworth, 2000] to relocate ~2700 high-frequency brittle-failure earthquakes (M ≤3.4) that occurred beneath Mammoth Mountain and describe the spatial-temporal evolution of the seismogenic structures activated during the 1989 earthquake swarm. Initially, a series of M<2 earthquakes occurred beneath the southwest flank of the volcano at a depth of ~6 km. About eight days later, earthquakes occurred at depths of 8 to 10 km ~1 km to the south, which over the next several weeks defined a vertical, tabular-shaped "keel" at 7-10 km depth that extended ~2 km to the

north-northeast beneath the southern flank of the mountain. By mid-October, seismicity in this keel largely died away and activity in the initial cluster at 6 km evolved into a ring-like pattern beneath the southern and western flanks of the volcano. This seismicity front moved circumfrentially away from its initiation point over the seismicity keel. In early June, seismicity migrated to shallower depths to define ring-like structures at 5-3 km and <3 km depth. The lower seismicity ring was conical in shape at 5-6 km depth and had a diameter of ~2.5 km concentric with the summit of Mammoth Mountain. Earthquake focal mechanisms in the deep seismicity keel were consistent with fluid intrusion into an opening crack [Hill et al., 1990; Prejean et al., 2003; Hill and Prejean, 2005]. Focal mechanisms for earthquakes defining the conical surface of the 5-6 km deep seismicity ring were consistent with uplift of Mammoth Mountain relative surrounding basement rocks.

Spasmodic bursts of high-frequency BF earthquakes with durations of tens of seconds to tens of minutes occurred frequently during the 1989 seismic swarm [Hill et al., 1990] and were likely associated with a rupture cascade through a fracture mesh caused by a transient increase in pore pressure. In addition, focal mechanisms for spasmodic burst earthquakes beneath Mammoth Mountain in 1997 recorded on a dense, temporary array of three-component seismometers were interpreted to reflect crack opening and fluid transport within a fracture mesh in the brittle crust [Foulger et al., 2004].

The rate of BF earthquakes in the upper 10 km of crust beneath Mammoth Mountain decreased to a low value by mid-1990. The most significant seismic swarm following the 1989 swarm occurred in September-December 1997 and included over 170 M>1.2 earthquakes beneath the edifice of Mammoth Mountain. Seismicity began at ~6 km depth and propagated to shallower depths at ~30 m/day. Most earthquakes occurred at 5-6 km depth and within the eastern limb of the 1989 lower seismicity ring.

A sequence of deep (10-25 km) LP earthquakes was recorded beneath Mammoth Mountain, the first in July 1989 [Pitt and Hill, 1994; Hill and Prejean, 2005]. The LP earthquakes likely occurred beneath the brittle-plastic transition where temperatures are >350-400^{o}C [Hill, 1992]. The rate of LP activity increased gradually from 1989-1990 through 1996 and then rapidly in 1997 (Figure 2.2A), preceding the 1997 seismic swarm by eight months. Hypocentral locations for LP earthquakes recorded by temporary deployment of 3-component seismic stations in 1997 show that LP earthquakes were located at that time within a narrow zone beneath the southwest flank of Mammoth Mountain and the seismicity keel of the 1989 swarm.

Three VLP volcanic earthquakes were also recorded beneath Mammoth Mountain in October 1996, and July and August 2000 [Hill et al., 2002]. One or more local LP earthquakes occurred concurrently with each of the VLP events and spasmodic bursts accompanied the July and August 2000 VLP events. The VLP earthquakes were loosely constrained to a source volume centered ~3 km beneath the summit of Mammoth Mountain, in the vicinity of a CO_2 reservoir proposed by Sorey et al. [1998] (see conceptual model section below). These data may reflect the transport of a slug of fluid (most likely CO_2 or a CO_2-rich hydrous phase) through a near-vertical, northwest-striking crack [e.g., Hill and Prejean, 2005]. Hill et al. [2002] suggested that the spasmodic bursts represent cascading shear failures in a fracture mesh surrounding the VLP source related to a local increase in pore pressure as the fluid slug moves through the crack. The

associated LP events would then represent triggered resonance of a two-phase fluid filling partially open cracks.

Dilation strain measurements by a borehole dilatometer showed that aseismic strain began two weeks before the 1989 seismic swarm [Langbein et al., 1993]. An extensional strain excursion of ~0.5 x 10^{-6} began on April 20 and ended with the beginning of the seismic swarm on May 2. This was followed by a ~0.2 x 10^{-6} compressional strain recovery that ended on May 10 when the seismic activity began in the 7-10 km-deep seismicity keel. A second compressional strain excursion of ~0.3 x 10^{-6} occurred from June 10 to 21, which was followed by gradual extensional strain into 1990. Leveling and electronic distance meter data showed small deformation (1-2 cm) and strainchanges associated with the 1989 seismic swarm [Langbein et al., 1993; 1995]. These changes were modeled by a crack dislocation centered beneath Mammoth Mountain that was coplanar with the seismicity keel.

Mammoth Mountain fumarole (MMF) is a thermal feature located at an elevation of 3030 m on the upper northern flank of Mammoth Mountain (Figure 2.3). From 1982 to July 1989, diffuse seepage of gas and steam were observed over a ~50 m^2 area of elevated ground temperatures and no distinct steam vents were observed within this area [Sorey et al., 1993]. In September 1989, distinct steam vents were observed and steam velocities from the ground had increased significantly. An increase in $^3He/^4He$ ratios measured in gases collected from MMF was observed following the onset of the 1989 earthquake swarm beneath Mammoth Mountain [Sorey et al., 1993]. For example, the $^3He/^4He$ value increased by 58% (i.e., to 5.45 R_A, where R_A is the atmospheric $^3He/^4He$ ratio) from August to September 1989, and then continued to increase to a maximum value of 6.72 in July 1990 (Figure 2.4). For reference, ratios typically range from 6 to 8 R_A for fluids from hydrothermal systems in continental magmatic systems. $^3He/^4He$ values have continued to show an elevated magmatic helium component since the 1989 swarm. $\delta^{13}C$ values of MMF CO_2 increased from –5.3‰ in July 1989 to –4.5‰ in August 1991, probably due to an increase in the magmatic CO_2 component in fumarolic gases [Sorey et al., 1993]. Overall, carbon and helium isotopic values likely indicate contribution of CO_2 from magmatic degassing and degassing of metasedimentary rocks.

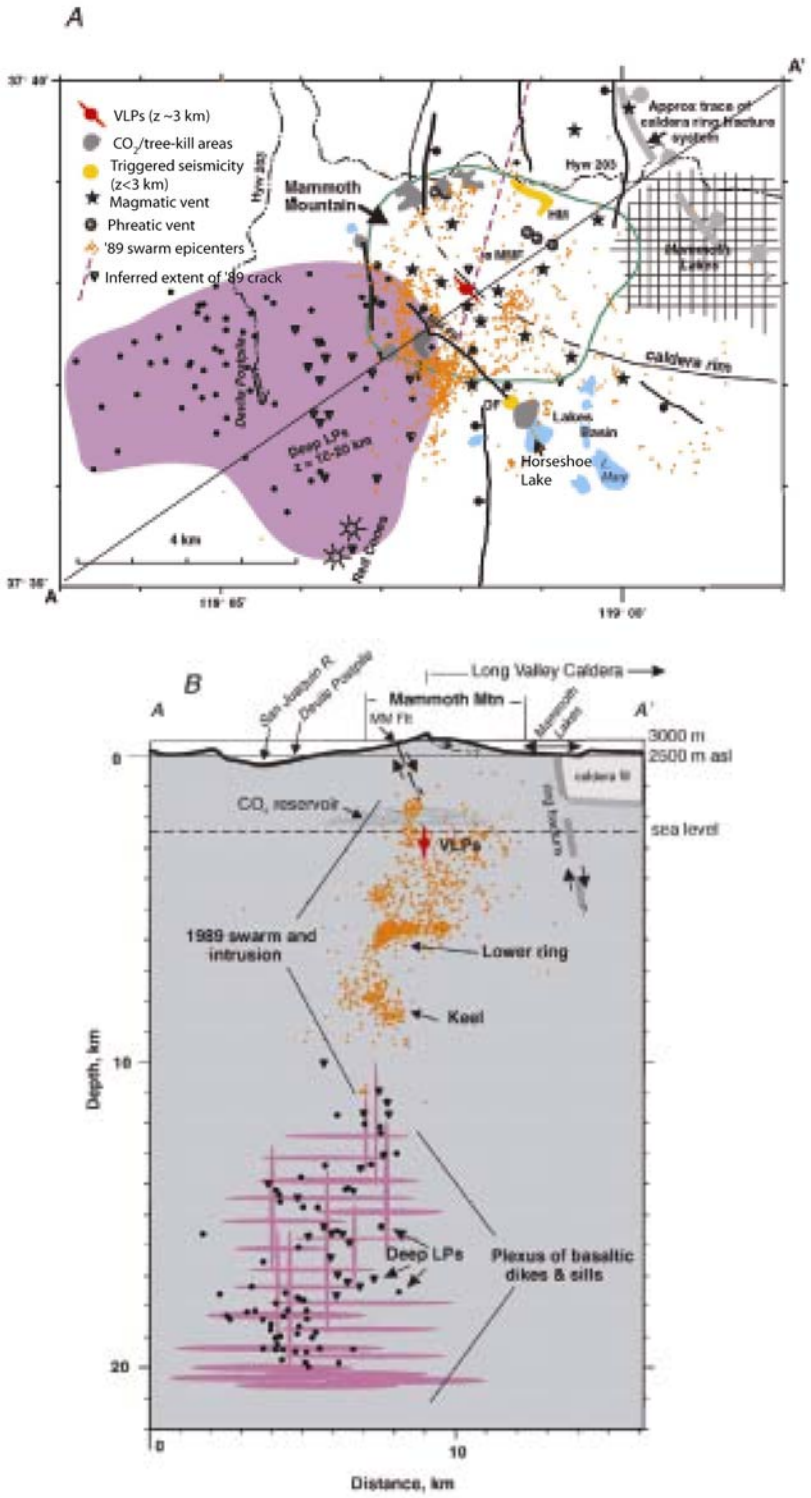

Figure 2.3. (A) Map of Mammoth Mountain (surrounded by a green line) and surrounding area with major faults (heavy black lines) (from Hill and Prejean [2005]). (B) Cross section A-A' showing faults with sense of slip (arrows), location of CO_2 reservoir proposed by Sorey et al. [1998], and plexus of dikes and sills. Orange dots, black dots, and triangles show hypocentral locations of BF earthquakes, locations of 1990-1999 LP earthquakes recorded

by NCSN seismic network [Pitt et al., 2002], and 1997 LP earthquakes recorded by temporary array of 3-component digital seismic stations [Foulger et al., 1998].

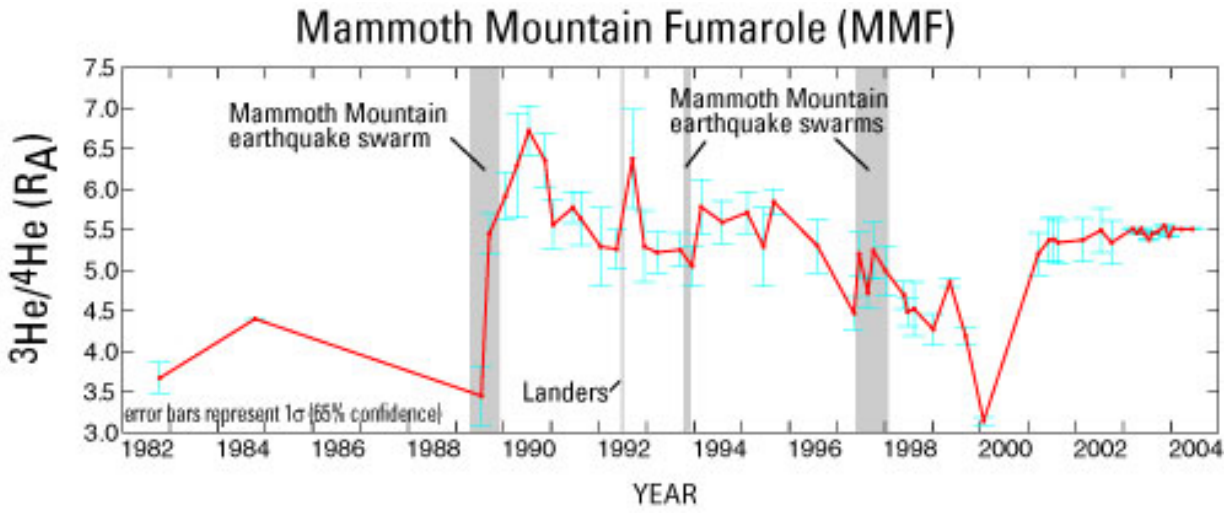

Figure 2.4. $^{3}He/^{4}He$ ratios versus time at the Mammoth Mountain fumarole [http://lvo.wr.usgs.gov/helium.html].

Trees were killed in six general areas (~360,000 m^2) on Mammoth Mountain in 1990-1991 (Figure 2.3). Also, during the winter of 1990, a park ranger in the Horseshoe Lake area exhibited signs of CO_2 asphyxiation. A series of soil and aerial gas flux surveys were conducted following these events and it was estimated that at least 250 metric tons of CO_2 per day (t d^{-1}) were emitted through soils from an approximately 480,000-m^2 area on the volcano [Farrar et al., 1999; Gerlach et al., 1999]. The areas of diffuse degassing appeared to be loosely correlated with the locations of mapped faults (Figure 2.3). Based on data (1996-1999) for cold springs discharging around Mammoth Mountain, Evans et al. [2002] estimated that the total discharge of magmatic carbon in the cold groundwater system was ~20,000 t yr^{-1}. They also suggested that the long-term discharge prior to the 1989 seismic swarm was ~10,000 t yr^{-1}. Areas of diffuse CO_2 emissions reflect zones of gas upflow where groundwaters are saturated with respect to CO_2.

The Horseshoe Lake tree kill area, located adjacent to Horseshoe Lake on the southeast flank of Mammoth Mountain (Figure 2.3) is the most studied of the areas of diffuse CO_2 degassing on Mammoth Mountain. Here, soil gas CO_2 concentrations measured using infrared gas analyzers are commonly >30 vol.% and fluxes measured using the accumulation chamber method are commonly >500 g $m^{-2}d^{-1}$ [Farrar et al., 1995, 1999; Rahn et al., 1996; McGee and Gerlach, 1998; Sorey et al., 1998; Gerlach et al., 2001]. For reference, background CO_2 concentrations and fluxes outside of the tree-kill area are usually < 1 vol.% and 25 g $m^{-2}d^{-1}$, respectively. Repeated measurements of soil CO_2 fluxes were made over grids from 1997 to 2000 and maps were contoured for soil CO_2 flux (e.g., Figure 2.5). Based on these data, total CO_2 emission rates were estimated to be 93 ± 27 t d^{-1} [Rogie et al., 2001]. An example of total CO_2 emission rate estimates versus time for the Horseshoe Lake tree kill area is shown in Figure 2.6 and does not show evidence of a sustained increase or decrease in CO_2 emissions from the Horseshoe lake tree kill area over this period of time [LVO Annual Report, 2002]. However, based on measurements of ^{14}C in tree rings around the Horseshoe Lake tree kill area prior to 1997, CO_2 emissions likely

began here in 1990, peaked in 1991, and declined by a factor of ~2 through 1998 [Cook et al., 2001].

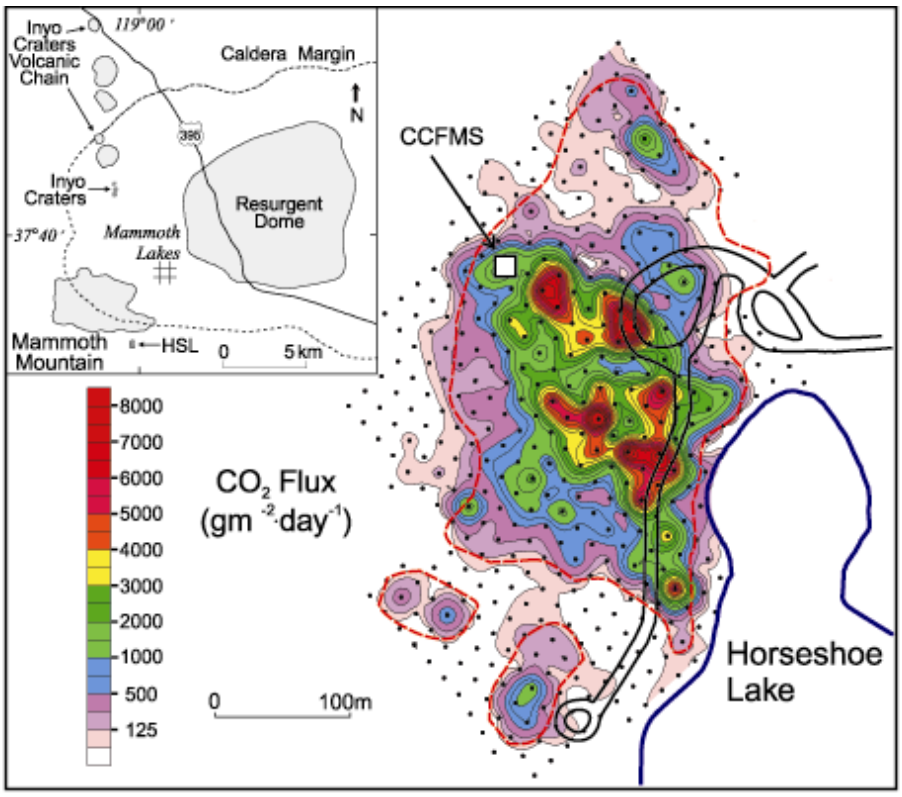

Figure 2.5. Map of the Horseshoe Lake tree kill area contoured for soil CO_2 flux (from Rogie et al. [2001]).

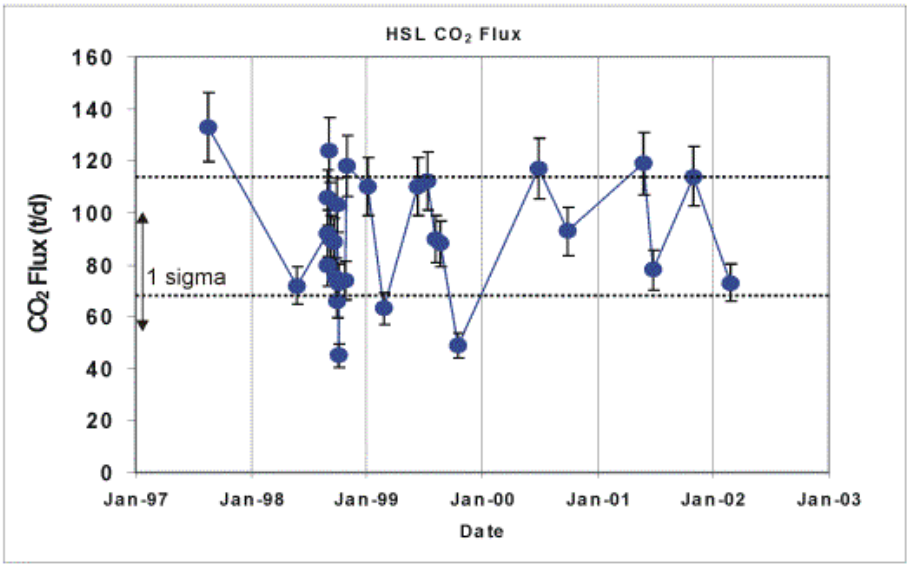

Figure 2.6. CO_2 emission rate versus time for the Horseshoe lake tree kill area from 1997 to 2000 [LVO Annual Report, 2002].

Continuous monitoring of soil CO_2 concentrations concurrently with meteorological parameters was carried out in the Horseshoe Lake tree kill area (e.g., Figure 2.7). These data show annual cycles of CO_2 buildup beneath winter (December-June) snow pack and decline during the springtime, to remain relatively constant through the summer and fall (Figure 2.7) [McGee and Gerlach, 1998; McGee et al., 2000].

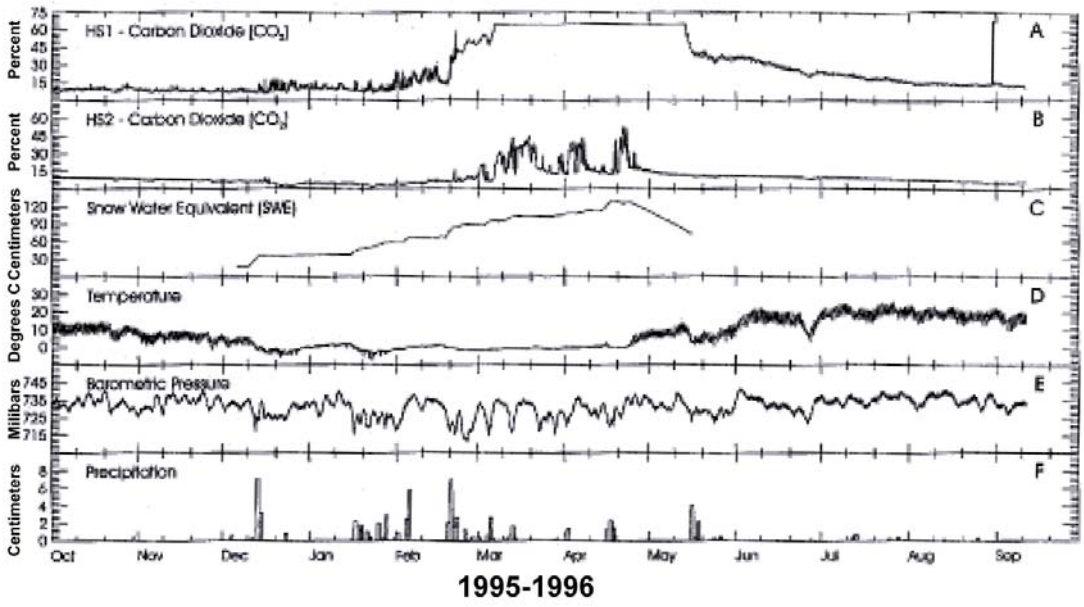

Figure 2.7. Time series of Soil CO_2 concentration (measured at stations HS1 and HS2) and meteorological parameters from 1995 to 1996 (from McGee and Gerlach [1998]). Plot A shows CO_2 concentrations off the gas analyzer measurement scale during wintertime months.

A continuous soil CO_2 flux monitoring station was also deployed in the Horseshoe Lake tree kill area from 1998 to 2000 and measured soil CO_2 flux concurrently with meteorological parameters [Rogie et al., 2001]. Spectral analysis of time series of data showed that temporal variations in CO_2 flux over this time period were strongly controlled by meteorological parameters (e.g., barometric pressure), rather than changes in processes at depth (Figure 2.8).

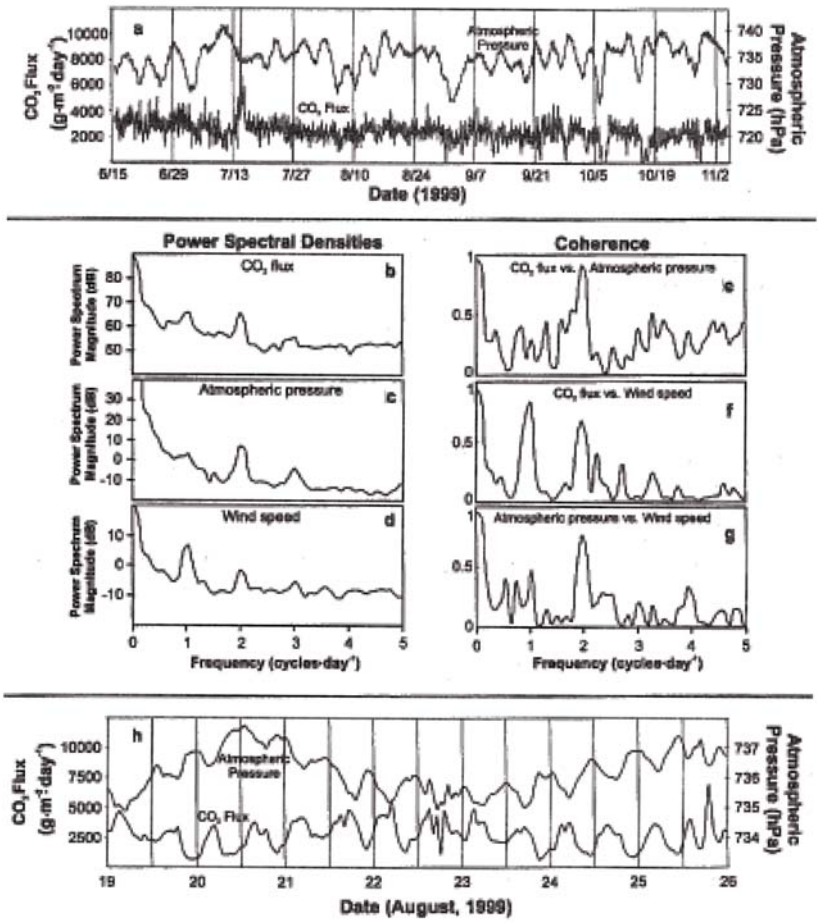

Figure 2.8. (a) Plot of soil CO_2 flux and atmospheric pressure versus time (June 15-November 4, 1999). Power spectra for (b) CO_2 flux, (c) atmospheric pressure, and (d) wind speed. Coherence spectra for (e) CO_2 flux versus atmospheric pressure, (f) CO_2 flux versus wind speed, and (g) atmospheric pressure versus wind speed. (h) Plot of soil CO_2 flux and atmospheric pressure versus time (August 19-26, 1999) (from Rogie et al. [2001]).

Conceptual model of structure, recent activity, and gas leakage. Based on available geophysical, geochemical, and hydrogeologic data, Hill and Prejean [2005] proposed a model of structure, recent unrest, and gas leakage at Mammoth Mountain. While perhaps speculative, this model is based on the most comprehensive data set for Mammoth Mountain to date. We excerpt from their discussion in this section, and for further details, the reader is referred to Hill and Prejean [2005].

The deep LP earthquakes observed beneath the southwest flank of Mammoth Mountain are likely associated with CO_2-rich fluids from basaltic dikes and sills located at 10-25 km depth (Figure 2.3). These dikes and sills are probably related to the field of mafic vents surrounding Mammoth Mountain. The plastic-brittle transition of crustal rocks likely coincided with the maximum focal depths (6-10 km) for BF earthquakes beneath Mammoth. Activation of the seismicity keel within this transition zone during the 1989 swarm was probably due to elevated strain rates associated with injection of magmatic fluids.

Swarms of BF earthquakes at shallower depths (to within a km of the surface) defined a series of ring-like structures concentric about the summit of Mammoth Mountain. Key characteristics of the earthquake swarms were consistent with brittle processes driven by elevated pore pressure and fluid transport. Based on volume and geochemical constraints, Sorey et al. [1998] proposed the existence of a 150^{o}C, high-pressure gas reservoir within the upper three km of the crust beneath Mammoth Mountain. The existence of the reservoir is also supported by the source volume for the VLP earthquakes of 2000 and 2001 [Hill et al., 2002]. The gas reservoir may occupy up to 20 km^3 of porous/fractured rock (although smaller volumes also satisfy flux and geochemical models), is capped by a low-permeability rock unit or hydrothermally altered zone, and is probably underlain by a higher temperature liquid water reservoir [Sorey et al., 1998]. The liquid reservoir likely scrubs more soluble magmatic gases (e.g., SO_2, HCl), leaving CO_2 as the main gas component in the gas reservoir. CO_2 within the reservoir has likely accumulated over an extended period of time fed by volatiles leaking up from the mid-crustal dikes and sills. Seismicity in the upper 3 km of the crust falls along the trends of the surficial structures mapped on the edifice of Mammoth Mountain. For example, the dominant earthquake cluster at ~3 km depth in the 1989 swarm was subparallel with the normal, northwest-striking, northeast-dipping Mammoth Mountain fault (Figure 2.3); these earthquakes may reflect slip on the lower segment of this fault.

Recent unrest at Mammoth Mountain has likely been driven by periodic releases of CO_2-charged magmatic fluids from basaltic magma bodies at mid-crustal depths and their ascent to shallow crustal depths. In the case of the 1989 swarm, onset of fluid mobilization was reflected as a dilatational strain signal on the dilatometer beginning in mid-April ~two weeks before the beginning of the swarm. The onset of BF earthquakes near the base of the brittle crust at ~6 km depth on May 2 was probably due to an increase in pore pressure as the diffusive leading edge of the fluid volume reached the base of the brittle crust. Brittle failure within the underlying brittle–plastic transition zone (the seismicity keel) 8 days later may have occurred as the bulk of the ascending fluid moved through the 10- to 7-km depth interval. As the ascending fluid reached the base of the brittle crust, it likely spread out in a sill-like pattern. Movement of fluid into the brittle crust probably caused the period of accelerating seismicity from mid-May through mid-July. Seismicity initiated at 5–6 km depth and moved circumferentially both clockwise and counter clockwise in the horizontal plane at ~0.5 km/month to define the lower seismicity ring. In early June, seismicity began propagating to shallower depths at a rate of ~1.7 km/month. The space-time progression of the seismicity fronts was consistent with the onset of earthquake activity being triggered by the diffusive propagation of a fluid pressure front.

The upwardly migrating seismicity front reached the upper 3 km beneath Mammoth Mountain between late August and early September. The CO_2-charged fluid then likely began pressurizing the shallow, pre-existing CO_2 reservoir proposed by Sorey et al. [1998]. The low permeability reservoir caprock may then have ruptured due to a combination of increasing pressure and seismicity allowing CO_2 gas to migrate to the surface. The CO_2 appeared at the surface in the form of diffuse CO_2 degassing in February 1990 [Sorey et al., 1998].

A pressure drop likely occurred within the mid-crustal dikes and sills as fluids were released from its upper portion. A pressure drop would trigger additional ex-solution of volatiles from the magma and possibly the injection of new basaltic magma into the plexus from depth, both contributing to the start of LP earthquake activity within the plexus. Mid-crustal LP earthquakes

and diffuse CO_2 degassing at a sustained rate at the surface have continued at Mammoth following the 1989 earthquake swarm. This suggests that CO_2 continues to leak from the shallow reservoir, which could potentially be replenished by volatile influx from depth. The 1996 and 2000 VLP earthquakes were probably caused by migration of discrete slugs of CO_2 or a CO_2-rich hydrous fluid discharged from the shallow reservoir along a crack into a shallow fracture mesh; a similar process was likely occurring during the later (shallow) phase of the 1989 swarm.

Hazards and Mitigation Techniques. The national forest and ski resort are popular recreation areas on Mammoth Mountain. As a result, high CO_2 levels in areas of diffuse CO_2 degassing pose a potential risk to the health and safety of people using the area for, e.g., skiing, hiking, and fishing. During the wintertime, snow levels accumulate and toxic levels of CO_2 can develop in snow wells (depressions) around trees and buildings, and immediately below the snow surface in areas of high CO_2 emissions [http://lvo.wr.usgs.gov/CO2.html]. Apart from the Forest Service employee who exhibited signs of CO_2 asphyxiation, one skier apparently died from CO_2 asphyxiation in a snow well near Horseshoe Lake [Hill, 2000], highlighting the potential danger of high CO_2 concentrations in the near-surface environment during winter months. During the summertime, it is hazardous to dig holes in and around areas where the trees have been killed by carbon dioxide gas. The natural collapse pits that have developed on the northwestern shore of Horseshoe Lake as the lake level declines contain high CO_2 concentrations; people (and pets) are warned against entering these pits or digging up loose soil that has been placed in the pits. People are also warned to avoid a crack 1-2 feet wide that extends from the lake onto the west shore and not to lie face down on the ground near Horseshoe Lake or the tree-kill area [http://lvo.wr.usgs.gov/CO2.html]. In addition to the public education that is ongoing at Mammoth Mountain, the U.S. Geological Survey continuously monitors the CO_2 concentrations in soils on Mammoth Mountain [http://volcanoes.usgs.gov/About/What/Monitor/Gas/continuous.html].

Lessons learned. Several lessons can be learned from the large release of CO_2 at Mammoth Mountain, CA and applied to risk assessment associated with geologic carbon storage. First, CO_2 can both accumulate beneath, and be released from, a gas reservoir with a capping unit with sealing capacity that can become compromised due to geomechanical damage. The potential exists for processes such as seismic activity or over pressurization of the storage reservoir to cause this geomechanical damage, and trigger the release of CO_2 from the reservoir. Next, unsealed fault and fracture zones can act as fast and direct flow paths for CO_2 from depth to the surface. Finally, risk to human health and safety from high CO_2 levels in the near-surface environment can potentially be mitigated based on public education and comprehensive CO_2 and geophysical monitoring programs.

2.2.3. Solfatara, Italy

Geologic Background. Solfatara volcano is located within Campi Flegrei, a 12-km wide caldera complex, located to the west of Naples, southern Italy (Figure 2.9). Campi Flegrei was formed in the eruptions of the Campanian Ignimbrite (37 ka) and the Neopolitan Yellow Tuff (12 ka) [Rosi and Sbrana, 1987; Orsi et al., 1996]. More recent volcanic activity in Campi Flegrei has been dominated by magmatic and hydromagmatic eruptions from 10,500 years ago to the 1538 eruption at the Monte Nuovo cone. Solfatara is a tuff cone consisting of ash and lapilli

beds overlying breccia and was formed between 3.8 and 4.1 ka [Rosi and Sbrana, 1987] (Figure 2.9). Hydrothermal eruptions occurred at Solfatara during the 12th century [Rosi and Santacroce, 1984]. The tuff cone is hydrothermally altered and is cut by two major normal faults striking NW-SE and fractures striking NE-SW and NW-SE (Figure 2.9).

Recent Activity. Two major (1969-1972 and 1982-1984) and two minor (1988-1989 and 1994) periods of resurgent uplift occurred in the Neopolitan Yellow Tuff caldera and define Campi Flegrei's most recent activity (Figure 2.9). The two major episodes of "bradyseismicity" generated earthquake swarms and net uplift of 3.4 m [Corrado et al., 1977; Barberi et al., 1984]. The 1982-1984 bradyseismic crisis was accompanied by 1.8 m of net uplift and over 16,000 earthquakes between 0 and 4 km depth, most of which were located in the Solfatara and Pozzuoli areas (Figure 2.9).

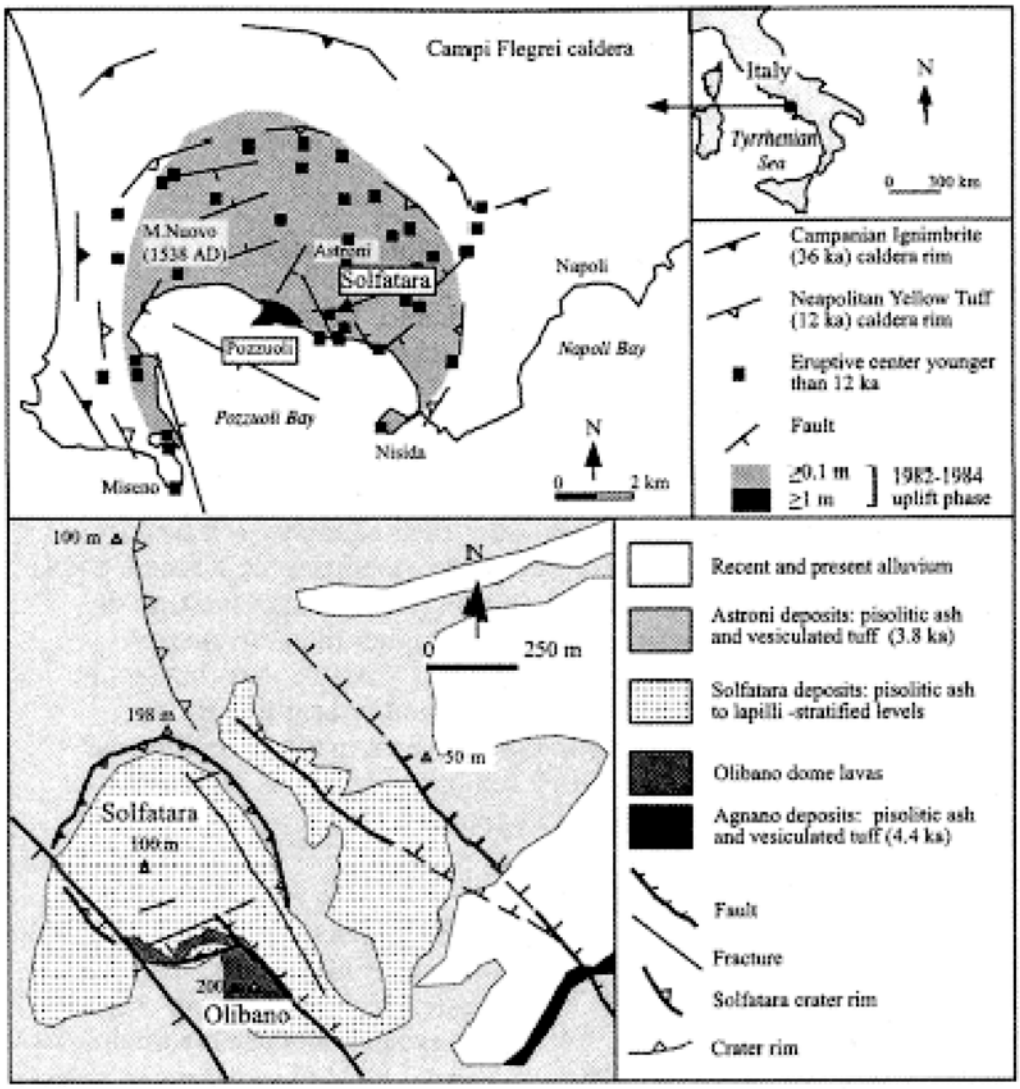

Figure 2.9. Maps of the structure of Campi Flegrei caldera (top) and the geology of Solfatara volcano (bottom) (modified from Chiodini et al. [2001]).

Extensive subaerial and submarine hot springs and fumaroles characterize current thermal activity in Campi Flegrei caldera [Allard et al., 1991]. The crater of Solfatara hosts the highest temperature fumaroles (140-160°C) of the caldera [Allard et al., 1991]. The geochemistry of fumarolic fluids has been used to develop a conceptual model of the hydrothermal system. The main components of the conceptual model (Figure 2.10) include: (1) a heat and fluid source supplied by a magma body at a few kilometers depth, (2) one or more boiling aquifers overlying the magma body, and (3) a fractured zone that is occupied by a gas phase ($T = 215^{o}C$, $P_{H2O} = 3.9$ bar, $P_{CO2} = 0.74$ bar) [Chiodini et al., 2001 and references therein]. This gas reservoir supplies a total mass emission rate of 4800 t d^{-1} and energy emission rate of 1.2×10^{13} J d^{-1} to the surface at Solfatara, primarily along major faults [Chiodini et al., 2001].

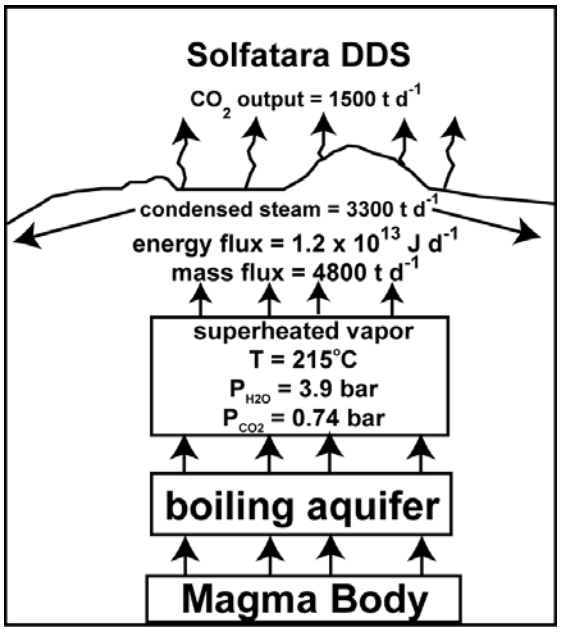

Figure 2.10. Conceptual model of the Solfatara hydrothermal system, developed based on the chemical composition of fumarolic fluids and soil temperature and CO_2 flux measurements (modified from Chiodini et al. [2001]).

Changes in the chemistry of Solfatara fumarolic fluids were recorded prior to the 1982-1984 period of unrest, as well as prior to the minor events of 1988-1989 and 1994 [e.g., Cioni et al., 1984; Martini, 1986; Tedesco, 1994; Tedesco and Scarsi, 1999]. For example, an increase in the H_2O/CO_2 ratio was observed prior to each of the episodes (Figure 2.11), indicating an increase in heat flow [e.g., Chiodini et al., 2001].

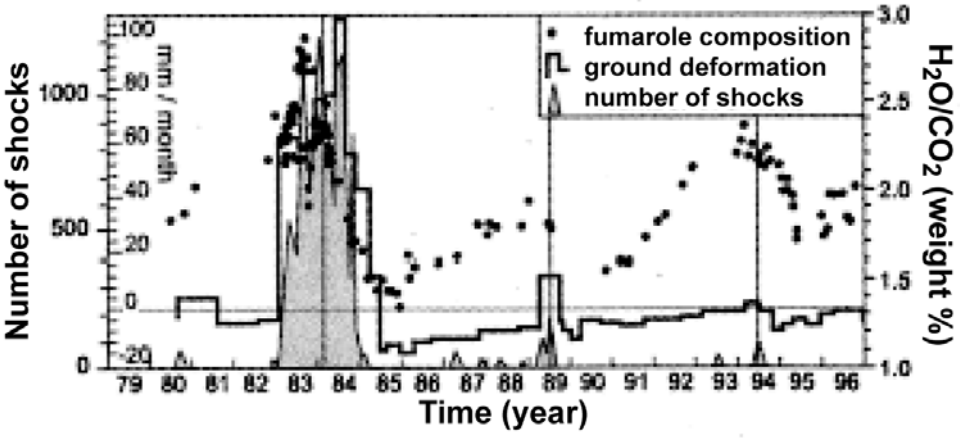

Figure 2.11. Plot of number of earthquake shocks, ground deformation, and H_2O/CO_2 versus time (modified from Chiodini et al. [2001]).

Also, increases in He, CH_4, H_2 and $^3He/^4He$ and decreases in ^{20}Ne, ^{40}Ar, and N_2 prior to the 1994 seismic swarm (e.g., Figure 2.12) were observed in Solfatara fumarolic gases and interpreted to result from migration of a relatively deep and hot gas phase to the surface and a decrease in the atmospheric gas component [Tedesco and Scarsi, 1999].

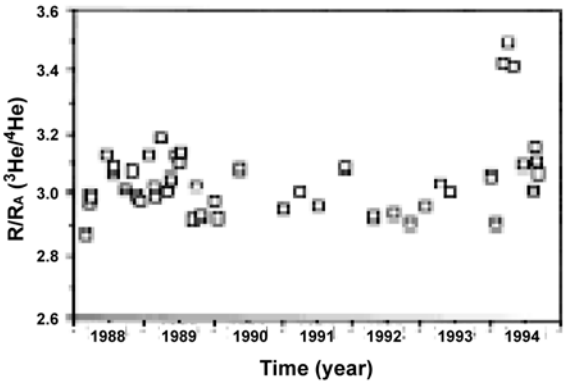

Figure 2.12. Plot of $^3He/^4He$ versus time for Solfatara fumarolic gases (modified from Tedesco and Scarsi [1999]) showing an increase in $^3He/^4He$ prior to the 1994 seismic swarm.

CO_2 Degassing at Solfatara. In addition to vent degassing, the crater of Solfatara hosts intense diffuse degassing of CO_2. Soil CO_2 fluxes have been measured using the accumulation chamber method at multiple locations within the crater; based on these measurements, maps of CO_2 flux have been produced (e.g., Figure 2.13) and used to estimate total CO_2 emissions from the area (~1500 t d^{-1} from a 0.5 km^2 area) [Chiodini et al., 2001]. Areas of elevated CO_2 flux (up to 52,000 g $m^{-2}d^{-1}$) are closely associated with faults and fractures; these permeable structures are interpreted to control gas flow to the surface [Chiodini et al., 2001]. Soil CO_2 flux has also been measured using the accumulation chamber method contemporaneously with meteorological parameters at two continuous monitoring stations in the crater (e.g., from 1997 to 2003; Figure 2.14). These time series of data show periodic fluctuations on CO_2 flux on diurnal to seasonal time scales. Soil CO_2 was not monitored during the episodes of seismic swarms and ground

deformation. The variations in gas chemistry, ground deformation, and seismic activity have been interpreted to result from overpressurization of the Solfatara hydrothermal system caused by an increase in magma degassing and/or sealing of the system due to argillification [e.g., Bonafede and Mazzanti, 1998; Chiodini et al., 2001].

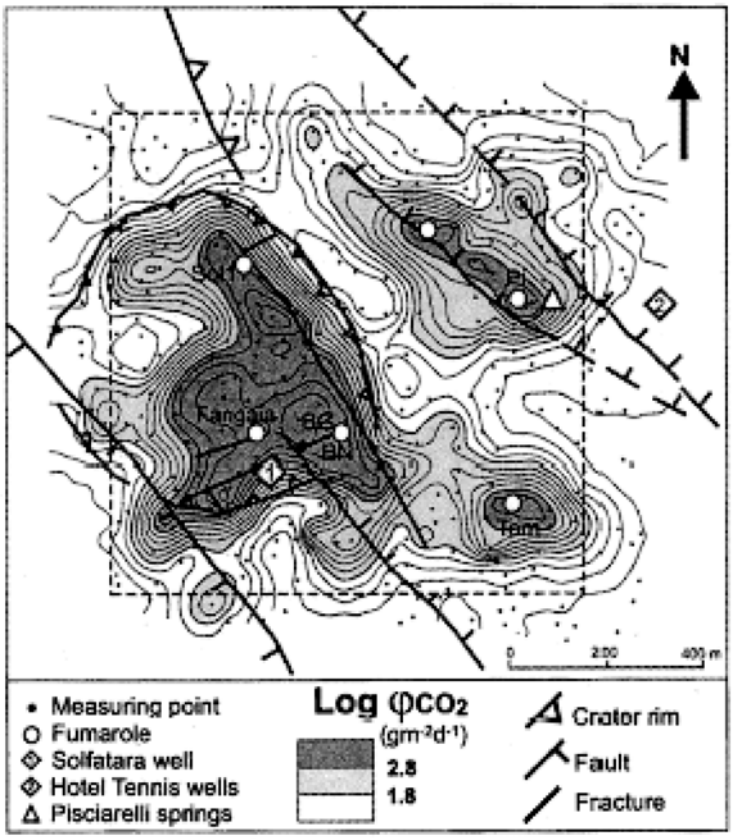

Figure 2.13. Map contoured for log soil CO_2 flux (φ_{CO2}) measured at Solfatara [Chiodini et al., 2001].

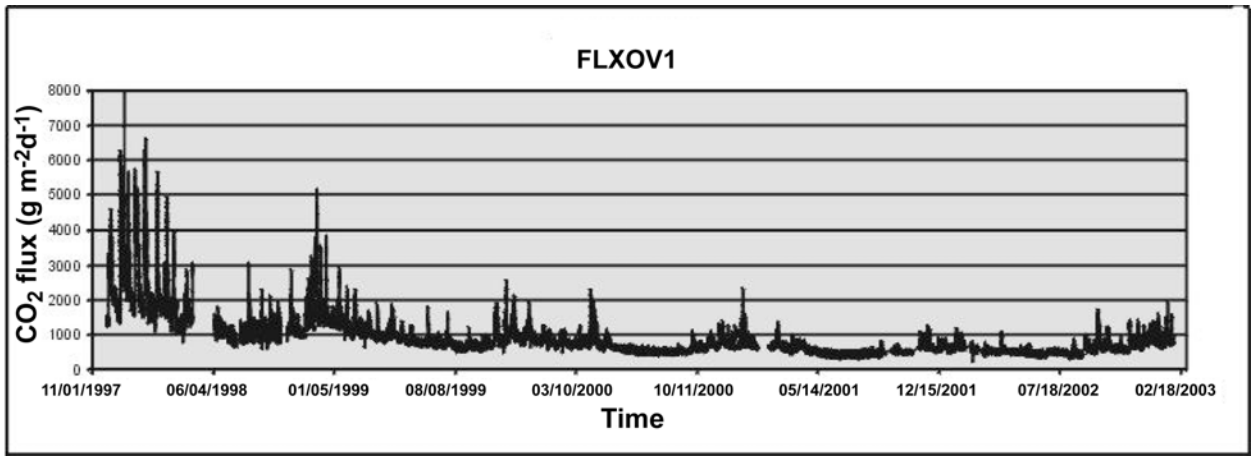

Figure 2.14. Time series of soil CO_2 flux measured at station FLXOV1 in Solfatara crater (modified from http://www.ov.ingv.it/geochemistry/flxov1.htm).

Hazards and Mitigation Techniques. Solfatara is a popular tourist destination and is surrounded by an intensely urbanized area. The area of diffuse CO_2 degassing in the crater of Solfatara lacks vegetation, likely due to the high soil CO_2 levels and/or temperatures. While no adverse human health effects or deaths associated with CO_2 degassing at Solfatara have been reported in the literature, the Osservatorio Vesuviano continuously monitors diffuse and vent degassing, including periodic sampling of fumarolic gases, periodic soil CO_2 flux measurements at regular locations within the crater, and continuous monitoring of soil CO_2 fluxes and meteorological parameters at two locations in the crater, in addition to geophysical monitoring (seismicity, gravity and deformation) [http://www.geowarn.ethz.ch/index.asp?ID=39]. Visitors to Solfatara are also warned about health hazards associated with the volcanic degassing.

Lessons learned. Several lessons can be learned from the large release of CO_2 at Solfatara volcano, Italy, and applied to risk assessment associated with geologic carbon sequestration. First, CO_2 can both accumulate beneath, and be released from, a gas reservoir with a capping unit with sealing capacity that can become compromised due to geomechanical damage caused by processes such as seismic activity or overpressurization. Next, unsealed fault and fracture zones can act as fast and direct flow paths for CO_2 from depth to the surface. Finally, risk to human health and safety from high CO_2 levels in the near-surface environment could be mitigated based on public education and comprehensive CO_2 monitoring programs.

2.2.4. Albani Hills, Italy

The Albani Hills (Figure 2.15) were constructed by explosive volcanism in an extensional tectonic regime and are composed of sequences of volcanic deposits (primarily alkaline-potassic lava flows and pyroclastic deposits) overlying sedimentary basement [Voltaggio and Barbieri, 1995; De Rita et al., 1995]. Ciampino is a city located 30 km southeast of Rome within the Albani Hills volcanic complex. CO_2 of magmatic and crustal origin is emitted at the surface in the form of diffuse soil, spring, and vent degassing at various locations throughout the Albani Hills and within the city of Ciampino [Annunziatellis et al., 2003; Beaubien et al., 2003] (Figure 2.15). Gas is hypothesized to leak up along major faults from deep pressurized reservoirs hosted by structural highs in carbonate basement rocks [Chiodini and Frondini, 2001].

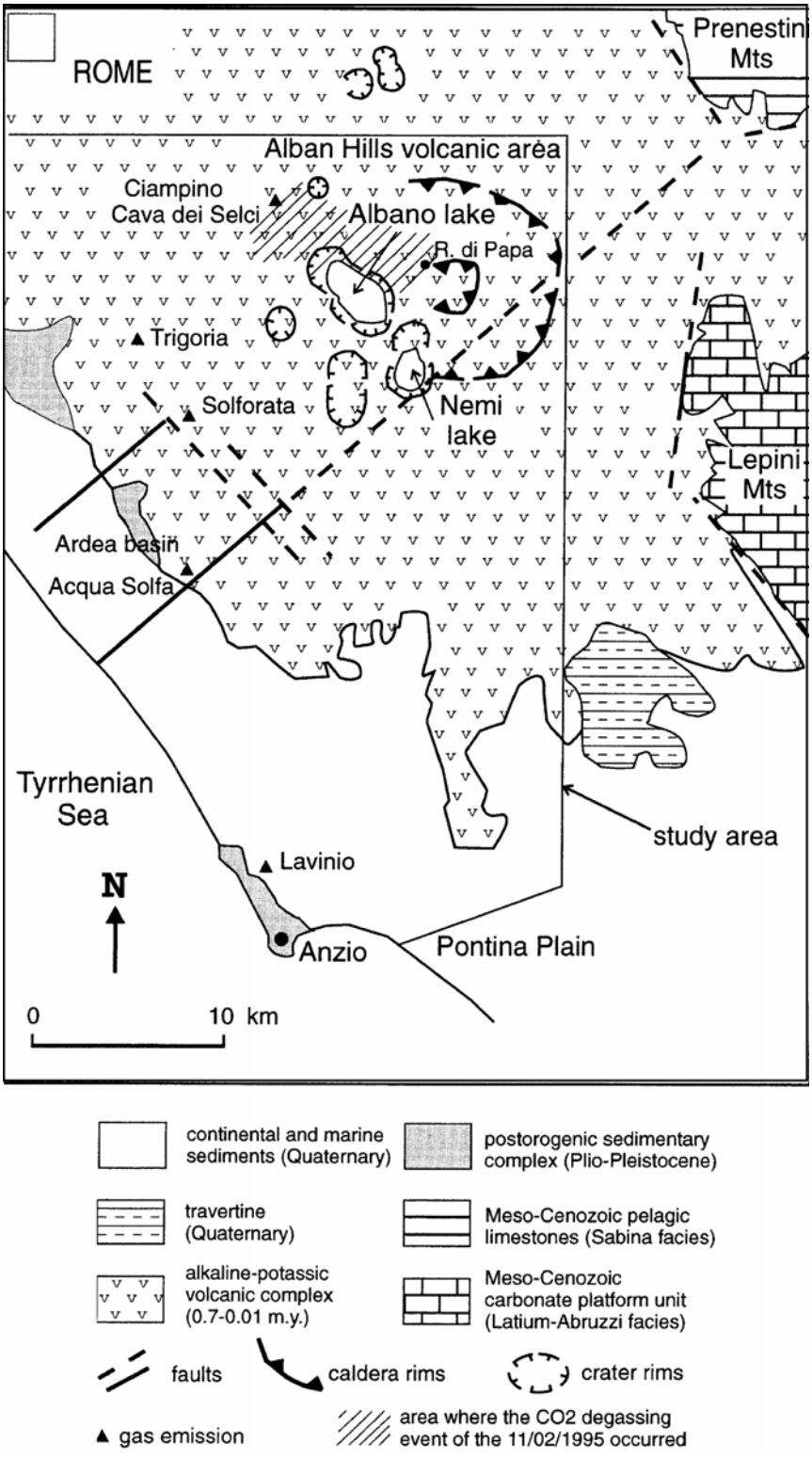

Figure 2.15. Geologic map of the Albani Hills region (modified from Chiodini and Frondini [2001]). The locations of the city of Ciampino, the 1995 CO_2 degassing event area, and the Cava dei Selci and Solforata CO_2 flux survey sites are shown.

A continual risk posed by soil and vent CO_2 degassing to the local population in Ciampino is the migration of CO_2 into unventilated basements of buildings and low-lying areas. Also, several large sudden releases of CO_2 have been recorded during historic times, the most recent of which occurred in 1995 and 1999. On November 2, 1995, a large area (25-km^2) of the Albani Hills was affected by the sudden release of CO_2 from the soil and shallow water wells. Residents reported noisy emissions of pressurized gas from the heads of shallow (< 60 m deep) water wells, and anomalous gas in basements. On the same day, researchers carried out field surveys and observed a well in Ciampino discharging lethal levels of CO_2 [Quattrocchi and Calcara, 1995]. The water had a pH of 5.48 and an alkalinity of 15.83 mmol l^{-1}, which increased and decreased, respectively, on November 3. Other wells in the Ciampino area showed similar trends in CO_2 degassing from November 2 to 3. Due to high CO_2 concentrations, basements of nearby buildings were inaccessible on November 2, but became accessible on November 3 as the CO_2 dissipated. Two low magnitude earthquakes occurred within 70 km of the study area on November 2 and 3; however, based on available data, the origin of the degassing event, its relationship to the earthquakes, and the total amount of CO_2 released are poorly understood. In September 1999, elevated CO_2 degassing occurred in conjunction with seismic activity, and 30 cows in a field within the city limits died as a result of CO_2 asphyxiation. It was hypothesized that the seismicty caused a decrease in the confining hydrostatic pressure and opening of faults, allowing for increased gas flow to the surface. Detailed descriptions of the 1995 and 1999 CO_2 releases can be found in Chiodini and Frondini [2001] and Beaubien et al. [2004].

Chiodini and Frondini [2001] measured soil CO_2 fluxes in 1996 at the Cava dei Selci area (6000 m^2) in Ciampino and the Solforata area (55,000 m^2) located southwest of Ciampino and observed elevated fluxes distributed along linear trends corresponding to prominent faults (Figure 2.16). They estimated total CO_2 emissions from these areas to be ~74 t d^{-1}. Beaubien et al. [2004] measured soil CO_2 concentrations in the Ciampino area ranging from 0.1 to 92.7 vol.%. Similar to CO_2 fluxes measured by Chiodini and Frondini [2001], they observed elevated CO_2 concentrations along linear trends paralleling major faults in the area, indicating that these structures provide pathways for upward gas migration. In addition, Chiodini and Frondini [2001] estimated the total rate of CO_2 dissolution into shallow ground waters to be ~506 t d^{-1} in the Albani Hills region. Although Beaubien et al. [2004] found that some houses were built on soils with CO_2 concentrations > 70 vol.%, a pilot study of indoor gas concentrations yielded CO_2 concentrations< 1 vol. %, likely due to the Italian custom of maintaining open windows in homes during the daytime. To minimize risk associated with elevated gas concentrations in homes, the University of Rome is working with the regional government and the local Civil Protection Agency to develop zoning bylaws, identify residential areas at risk, and develop education programs for residents.

We learn from the Albani Hills that CO_2 may accumulate in deep pressurized reservoirs within structural highs of sedimentary basement rocks. This CO_2 leaks to the surface along major faults. Sudden large releases of CO_2 from gas reservoirs may also occur as a result of seismic acivity that causes geomechanical damage. Also, the style of CO_2 release at the surface is highly variable, including discharge from wells, vents, springs, and diffusely through soils. Finally, the loss of human life due to elevated CO_2 levels in homes could be mitigated due to coordinated risk assessment and public education programs.

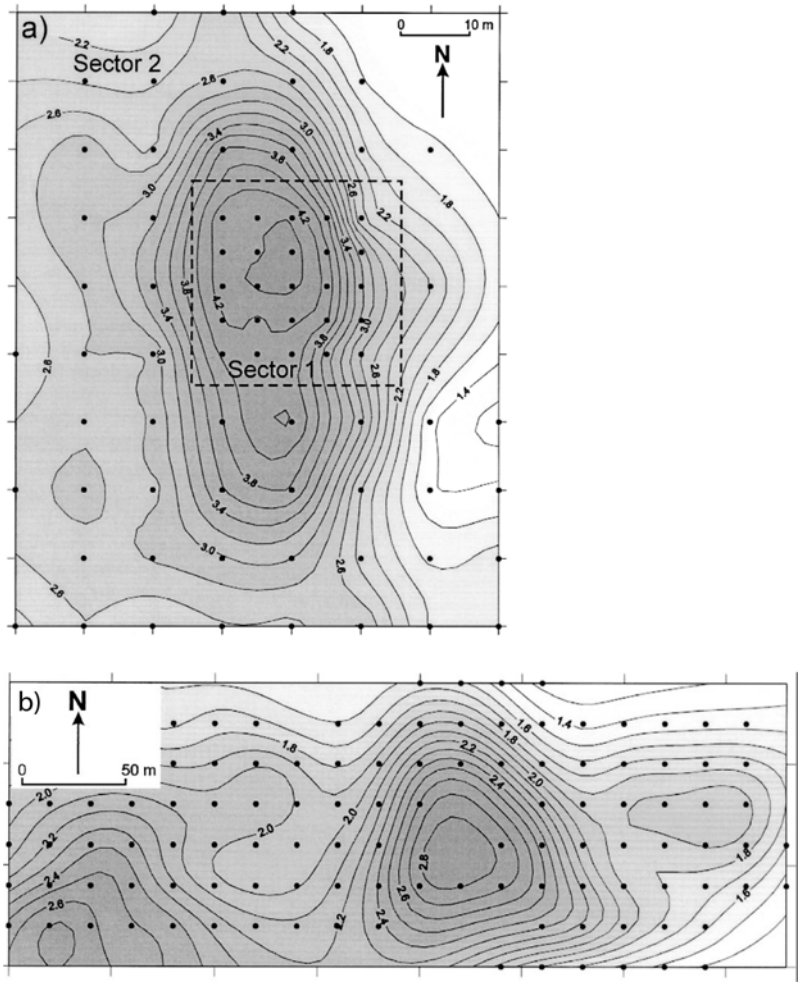

Figure 2.16. Maps contoured for log CO_2 flux (g m^{-2} d^{-1}) for the (a) Cava dei Selci and (b) Solforata areas in the Albani Hills region (modified from Chiodini and Frondini [2001]).

2.2.5. Clear Lake, California, USA

The Clear Lake volcanic-magmatic system is located in a rural area in northern California within a broad zone of deformation related to the San Andreas fault system. In this region, Coast Range ophiolite rocks and the Mesozoic Great Valley marine sedimentary sequence are thrust above coeval Franciscan Complex rocks (metamorphosed subduction zone metagraywackes and argillites) (Figure 2.17). These rocks are overlain by Tertiary marine and nonmarine rocks and late Pliocene to Holocene mafic to silicic Clear Lake Volcanics. Numerous strike-slip, thrust, and normal faults cut the region. The Clear Lake volcanic-magmatic system is thought to be related to the northward migration of the Mendecino triple junction and associated upwelling of the asthenosphere in a slabless window [e.g., Dickinson and Snyder, 1979; McLaughlin, 1981; Johnson and O'Neil, 1984]. Volcanism around Clear Lake is localized in regions transtension associated with structures of the San Andreas fault system.

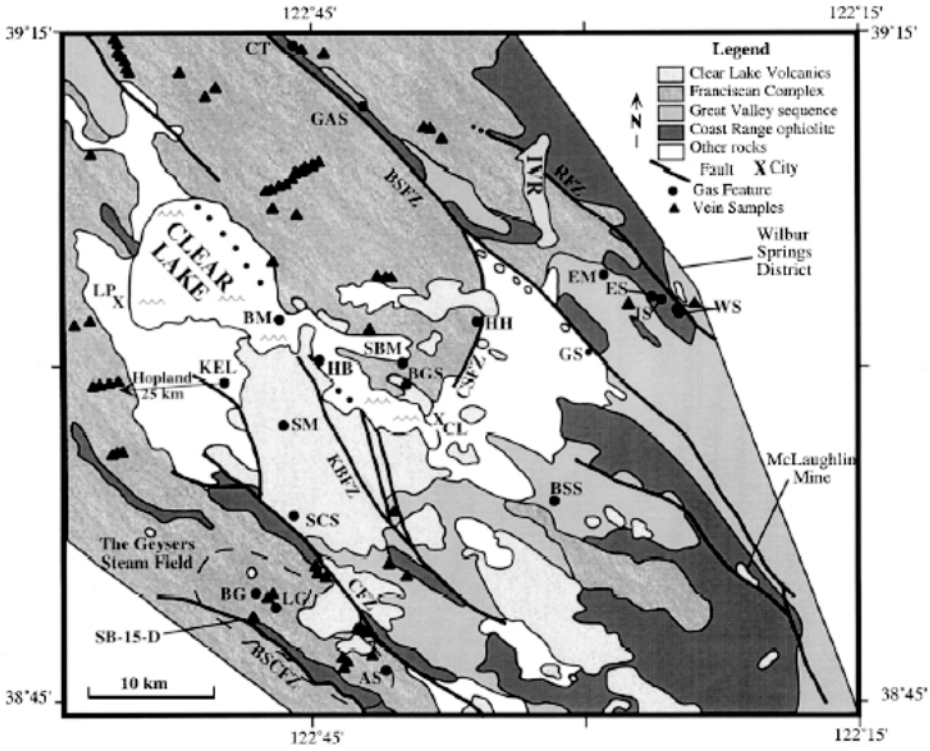

Figure 2.17. Generalized geologic map of the Clear lake area, northern California, with locations of surface gas features (vents and springs) (from Bergfeld et al. [2001]; Donnolly-Nolan et al. [1993]).

The Franciscan Complex hosts a geothermal system which includes several localized liquid-dominated reservoirs (e.g., Sulfur Bank Mine, SBM in Figure 2.17), with fluid temperatures up to 218°C at 503 m depth [Goff et al., 1995], the heat source for which is likely a large silicic magma body underneath the Clear lake volcanic field. There are numerous surface thermal features (e.g., thermal and mineral springs, gas vents) in the area (Figure 2.17). Many of the springs are CO_2 rich, discharge along fault zones, and deposit carbonate travertine [e.g., Goff et al., 1993a]. Most gases from thermal and non-thermal springs are composed of > 95% CO_2 [Bergfeld, 1997]. Based on isotopic analyses, CO_2 is primarily derived from thermal decomposition of metasedimentary rocks, with a minor contribution from magmatic sources [Bergfeld et al., 2001]. Gases from thermal features in the Clear Lake region range have 3He/4He ratios ranging from 0.8 to 7.9 R_A, with the highest values indicating a large mantle-derived He component [Goff et al., 1993b]. Bergfeld [1997] measured CO_2 fluxes from vents and soils (e.g., Sulfur Bank Mine) and estimated that up to one t d^{-1} of CO_2 is released at the surface from individual geothermal reservoirs. Bergfeld [1997] observed that CO_2 emissions were highly focused, with fluxes decaying rapidly with distance from gas vents. We learn from the example of Clear Lake that CO_2 is released from depth along major faults and results in a wide variety of styles of emissions at the surface.

One person was killed in 1912 as a result of "gas poisoning" when exploring an abandoned mining tunnel near the Bartlett Springs resort on Clear Lake [http://www.cagenweb.com/lake/lakobits.htm]. The tunnel was known to contain gas that had

previously killed small animals and birds. Also, three people have died (in 1878, 1981, and 2000) as a result of CO_2 asphyxiation when bathing in a Soda Springs, a popular mineral pool on an island near the shore of Clear Lake [e.g., The Press Democrat, 2000; http://www.sfgate.com/cgi-bin/article.cgi?file=/news/archive/2000/09/26/national0057EDT0406.DTL]. Gas concentration measurements made following the 2000 death showed that the air 6 to 8 inches above the water level was 60 % CO_2. The bath was subsequently closed to the public.

2.2.6. Latera Caldera, Italy

Latera caldera (8 x 11 km) is located in the Vulsini volcanic complex in Latium, central Italy. This volcanic complex is characterized by Quaternary alkali-potassic pyroclastic flows, pyroclastics, lavas, and cinder cones ranging in age from 1 Ma to 55,000 years old [e.g., Locardi et al., 1975; Varekamp, 1979]. Latera caldera hosts a water-dominated geothermal reservoir (200 to 230^{o}C) in metamorphosed carbonate rocks, the depth of which varies from 1000 to 1500 m [Cavarretta et al., 1985] due to faulting, folding, and uplift. CO_2 is the dominant gas in the geothermal reservoir [Cavarretta et al., 1985], the source of which is thermal decomposition of carbonate rocks and fluids associated with the dormant volcanic complex [Annuziatellis et al., 2004]. The reservoir is sealed by overlying hydrothermally altered volcanic rocks [Cavarretta et al., 1985].

CO_2 originating from the geothermal reservoir migrates vertically along major NW-SE and NE-SW trending fault zones and is emitted at the surface in Latera caldera in the form of diffuse soil, vent, and spring degassing. Soil and vent gas surveys have been conducted to measure CO_2 concentrations by gas chromatography; vent gases have CO_2 concentrations > 90%, and soil CO_2 concentrations range up to 97%, with an average value of 4.7% [Astorri et al., 2002]. These surveys have shown that elevated soil CO_2 concentrations and gas vents are restricted to small areas aligned along faults, indicating that gas flow is channeled along small gas-permeable pathways within the fault zones [Annuziatellis et al., 2004]. Vegetation is either lacking or is "stressed" in the areas surrounding gas vents [Annuziatellis et al., 2004]. Astorri et al. [2002] assessed hazards associated with gas emissions in the Vulsini volcanic complex using soil gas measurements, geological data, geostatistical analysis, and Geographic Information Systems to create a risk map of the area. The highest risk was associated with the central Latera caldera area where both major faults and minimum sediment overburden occur. Overall, we learn from the example of Latera caldera that CO_2 is released from a 1-1.5 km-deep reservoir with a hydrothermally altered capping unit. CO_2 migrates to the surface along major fault zones and is emitted in a wide variety of forms such as diffuse soil, vent, and spring degassing.

2.2.7. Mátraderecske, Hungary

Mátraderecske is a town in northern Hungary in the foreland of the Mátra Mountains, Middle Miocene andesite volcanoes. Here, andesite, andesite tuff, and andesite agglomerates are underlain by basement limestone and shale, and are locally overlain by clays and sands [e.g., Tóth et al., 1997]. Major faults striking NE-SW are seismically active. Deeply derived gases (e.g., CO_2, CH_4) associated with geothermal activity migrate from a karst water reservoir at ~1000 m depth upwards along the faults and fractures within the andesite, and then move both laterally and vertically along bedding planes and faults, respectively, in the overlying sediments.

Gas vents in Mátraderecske discharge CO_2, CH_4, and Rn and numerous CO_2-rich springs and wells are found in the area. CO_2 is used in medicinal 'spas'. Soil CO_2 fluxes have been measured up to ~1700 g $m^{-2}d^{-1}$, with average values of ~200 to 400 g $m^{-2}d^{-1}$ [NASCENT, 2005]. As a result of the CO_2 seepage, high CO_2 concentrations (up to 90 vol.%) can occur in basements of homes and have resulted in human deaths, the last of which occurred in 1995 [Tóth et al., 1997]. Residents of Mátraderecske have installed CO_2 detection devices and control systems (e.g., tubes and pumps) in homes to mitigate potential hazards [NASCENT, 2005]. Two homes were demolished in 1993 due to high CO_2 levels. The town supports an active public education program to inform residents and visitors of the hazards associated with CO_2.

2.2.8. Dieng Volcanic Complex, Indonesia

The Dieng Volcanic Complex in Java, Indonesia, is composed of two or more stratovolcanoes and numerous small craters and cones, overlying sedimentary sequences of limestone, sandstone, and shale. Major E-W and NE-SW striking faults control the location of volcanic centers. In February 1979, an eruption began at the pre-existing, water-filled Sinila crater where dark grey clouds and hot mudflows were emitted from the crater [Madjo, 1979]. Gas emissions ceased from Sinila crater two days after the initial eruption. A new crater was also created nearby and contained a 71°C fumarole. The low temperature of this discharge required the presence of a significant gas component for the vapor mixture to meet atmospheric pressure, leading Giggenbach et al. [1991] to propose that the eruptions were “pneumatic”, i.e., driven by gas at low temperature. A new fissure aligned with the two craters was also activated and on February 20, 1979, a cloud of gas, predominantly CO_2, was released from the fissure [Allard et al., 1989]. The gas was likely primarily of magmatic origin, based on stable carbon isotopic compositions of CO_2 and He/CO_2 ratios [Allard, 1989]. The gas cloud killed 142 people as well as several rescue workers.

2.2.9. Rabaul, Papua New Guinea

Rabaul is a pyroclastic shield volcano on New Britain Island, Papua New Guinea. Several large caldera-forming eruptions have occurred over Rabaul’s history and historial eruptions have formed intra-caldera cones [e.g., Newhall and Dzurisin, 1988]. Eruptive products range from basaltic to dacitic in composition. In June 1990, toward the end of a 51-year non-eruptive period at Tavurvur cone, CO_2 was released from a 25-m deep pit crater at Tavurvur. Three people were killed while attempting to collect bird eggs in the crater, and then three more people were killed when trying to rescue them. The release of CO_2 occurred suddenly (over the previous several days), as people collecting bird eggs in the crater a week earlier were unaffected. With the aid of SCUBA equipment, the bodies were recovered and a vent was found at the bottom of the crater wall from which gases were emitted at low temperature (48°C). The thickness of the CO_2 layer at the bottom of the crater was observed to vary between 1.7 and 4.8 m during the month following the deaths, and when windy, the CO_2 cloud was completely dispersed. High levels of CO_2 were also observed in Tavurvur’s crater in October 1981 when dead animals were discovered there [SI, 1990].

2.2.10. Lakes Monoun and Nyos, Cameroon

In 1984 and 1986, lethal gas bursts occurred at Lakes Monoun and Nyos, respectively, in Cameroon. These gas bursts have since been labeled as "limnic eruptions" [e.g., Tietze, 1987]. A limnic eruption occurs when a deep tropical lake becomes supersaturated with respect to CO_2 due to input of CO_2 into the bottom of the lake through volcanic degassing. Due to the increased bulk density of the bottom layer, large quantities of CO_2 can build up over years, leading to lack of seasonal turnover and a stably stratified lake. Under normal conditions, CO_2 may diffuse into shallow waters and escape gradually to the atmosphere as bubbles formed at shallow water levels. However, the rapid lake overturn triggered by a landslide, earthquake, strong wind, or cold descending rainwater can cause depressurization of CO_2-rich deep waters and nucleation of CO_2 in the deep water. Once the CO_2 begins to ascend, it becomes a self-sustaining fountain as CO_2-rich water is entrained with and pulled up beneath the ascending, expanding two-phase mixture.

Both Lakes Monoun (95-m deep) and Nyos (210-m deep) are located within the crater of an extinct volcano along the volcanic chain in the western highlands of Cameroon. At approximately 11:30 pm on August 15, 1984, people in villages nearby Lake Monoun reported hearing an explosive noise and feeling an earthquake. The following morning, a whitish cloud hung over the lake and surrounding area and people were found dead along the road near the lake with burns and skin lesions. Domestic and wild animals were also found dead in the area and vegetation was described as bleached and withered. A landslide scarp was observed from the eastern crater rim to the eastern lakeshore and vegetation at the east end of the lake was flattened, likely from a 5-m water wave caused by the displacement of lake water by the landslide. This landslide is hypothesized to have triggered the rapid turnover of Lake Monoun, leading to the limnic eruption and the deaths of 37 people. A detailed description of the events surrounding the eruption can be found in Sigurdsson et al. [1987].

In the case of Lake Nyos, the limnic eruption occurred without warning during the evening of August 21, 1986 and was associated with a degassing process lasting approximately four hours. The cause of rapid lake overturn has not been clearly identified. Extensive damage to vegetation and soils resulted from 20-80 m directional waves. 240,000 tonnes of CO_2 were lost from the upper 100 m of lake Nyos [Giggenbach, 1990] and the cloud of gas spilled over the crater rim, killing some people there. The gas flowed and accelerated down along two narrow valleys, preventing dispersion of the gas. Damage to vegetation was observed along the flow path of the gas and humans and animals in the cloud dropped unconscious, comatose, or dead almost immediately. The final toll was 1746 people, over 3000 cattle, and innumerable other animals, killed up to 27 km away and 24 hours after the initial gas release. Detailed descriptions of the Lake Nyos disaster can be found in e.g., Freeth and Kay [1987], Baxter and Kapila (1989), LeGuern et al. [1992], and Evans et al. [1994]. Today, in an effort to mitigate CO_2 buildup at depth and prevent future eruptions, researchers are degassing both Lakes Monoun and Nyos using vertical pipes extending from the lakes' surfaces to near the lakes' bottoms [e.g., Halbwachs et al., 2004]. These pipes activate controlled fountains of CO_2-water mixtures, safely venting CO_2 to the atmosphere.

We learn from the examples of Lakes Monoun and Nyos that under if a deep tropical lake is present into which CO_2 leaks from a deep source, CO_2 can build up, leading to lack of seasonal

turnover and a stably stratified lake. If a trigger mechanism then causes rapid lake overturn, a self-sustaining eruption of CO_2 can occur, releasing large and lethal quantities of CO_2 into the atmosphere. However, artificial degassing schemes where CO_2 is released in a controlled fashion to the atmosphere may help prevent the dangerous build-up of CO_2 in the lakes.

2.2.11. Laacher See, Germany

Laacher See is a lake-filled crater (2.5 x 1.8 km) in western Germany, formed ~11,000 years ago as a result of an explosive volcanic eruption [Schminke, 1989]. Laacher See is part of the East Eifel Volcanic Field, which overlies the Rhenish shield and Rhine Graben rift zone. Numerous CO_2-rich mineral springs are found throughout the Eifel region, and discharge of gas (~ 99 vol.% CO_2) is visible within the lake water and on the eastern shore of Laacher See. The lake is 51 m deep. Isotopic data indicate that the CO_2 is of deep mantle/magmatic origin [Griesshaber et al., 1992; Giggenbach et al., 1991]. A bubble flux of mantle-derived CO_2 in lake water was estimated to be 4 g $m^{-2}d^{-1}$ and the annual release of CO_2 to the atmosphere is about 5000 tonnes [Aeschbach et al., 1996]. The chemical composition and origin of gases in Laacher See are similar to Lake Nyos; as a result, concern has been raised that Laacher See may present a similar hazard from CO_2 buildup and subsequent catastrophic release [e.g., Giggenbach et al., 1991]. However, because annual lake turnover and vertical mixing occurs at Laacher See, the gases seeping into the lake bottom are released to the atmosphere at a much higher rate than they are at Lake Nyos and hazardous accumulation of CO_2 has been deemed unlikely [Aeschbach et al., 1996].

2.2.12. Paradox Basin, Utah, USA

The Paradox Basin, located in the Colorado Plateau area in southwestern Utah/southeastern Colorado, contains a number of actively producing oil, gas, and CO_2 fields. The Paradox Basin is filled with faulted and folded clastic and carbonate sedimentary rocks; its extent is defined by organic-rich Pennsylvania and Permian marine limestones, shales, and evaporates (Figure 2.18). The CO_2 reservoirs in the basin are vertically stacked and have accumulated within fault-bounded anticlines in sand-rich units that are also the dominant aquifers in the area. Shale or siltstone-rich capping units commonly provide seals.

Present day gas and water flow to the surface in the northwestern Paradox Basin is primarily controlled by the Little Grand and Salt Wash faults (Figure 2.18) that cut north-plunging anticlines and provide high-permeability pathways for fluid flow. These faults are part of a set of west-northwest trending 70-80^o dipping normal faults in the basin and show evidence for Early Tertiary and Quaternary slip [Shipton et al., 2004]. Active CO_2 leakage and seepage along these faults is characterized by CO_2-rich springs, travertine mounds, gas seeps, and leaky well bores (abandoned oil exploration and water wells; see Section 2.3.3). Fossil travertine mounds also run parallel to the Little Grand and Salt Wash fault traces, indicating extensive past CO_2-rich spring discharge. Based on stable carbon isotopic compositions, the source of the CO_2 is likely thermal decomposition of carbonate rocks [e.g., Heath, 2004; Shipton et al., 2004]. Helium isotopic data for gas from the Crystal Geyser (see Section 2.3.3 below) and a spring on the Salt Wash fault show evidence for only a minor contribution of mantle-derived gas [Heath, 2004]. Anomalously high surface CO_2 fluxes up to ~100 g m^{-2} d^{-1} have been measured using the accumulation chamber method along the Salt Wash faults, primarily within small localized areas

[Allis et al., 2005]. However, total CO_2 emission rates from soils and springs have not yet been quantified. No adverse effects of surface CO_2 discharge on people visiting the area or on ecosystems have been reported to date [Shipton et al., 2004]. Based on geological and geochemical data, Shipton et al. [2004] proposed a model of fault-controlled fluid flow in the northwestern Paradox Basin. The shallow Navajo/Wingate sandstone aquifer contains low temperature CO_2-rich waters from which surface spring and geyser discharges are sourced. While shale units cap the aquifer, the Little Grand and Salt Wash faults cut the sealing units, and allow for fluid to move in the vertical direction due to the high hydraulic conductivity. Lower cross-fault permeability relative to up-dip permeability causes the faults to act as barriers to cross-fault fluid flow.

We learn from the Paradox Basin example that CO_2 can accumulate in, and be released from, primary and secondary high-permeability sedimentary units capped by low-permeability units. CO_2 migrates vertically between reservoirs and to the surface along major faults to be released naturally as gas seeps, diffuse soil emissions, and spring emissions.

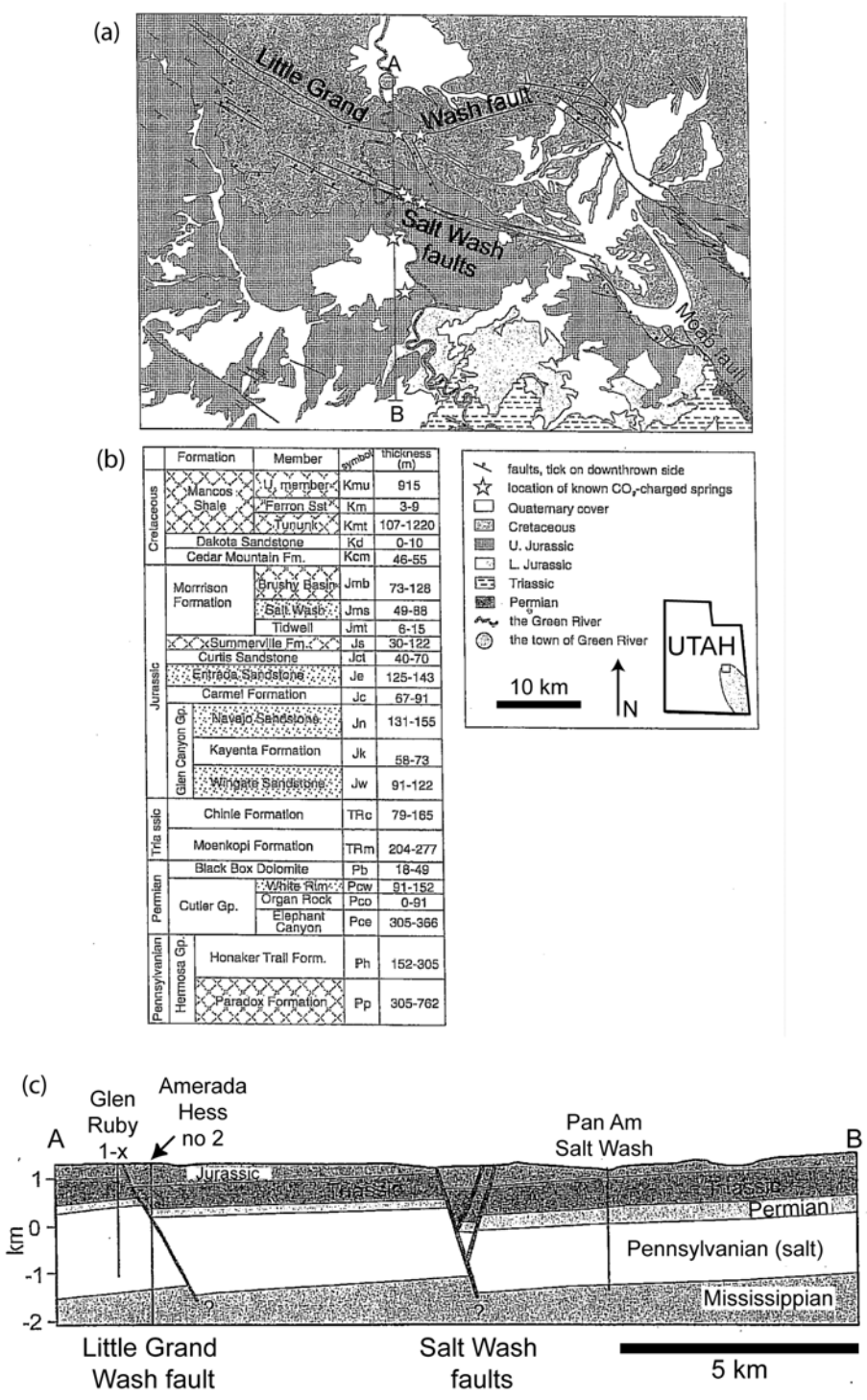

Figure 2.18. (a) Regional geology of the Little Grand and Salt Wash faults. Inset shows approximate area of Paradox basin. (b) Stratigraphic column. Stippled areas represent likely reservoir or aquifer rocks. Cross hatched areas represent cap rocks or seals. (c) Schematic cross-section across the Little Grand and SaltWash faults (see (a) for line A-B). Abandoned oil wells (projected onto line of section) give control on stratigraphy. Figure was modified from Shipton et al. [2004].

2.2.13. Florina Basin, Greece

The Florina basin lies within the northern area of a NNW-SSE-trending graben that extends150 km from northern Greece to the former Yugoslav Republic of Macedonia. This middle Tertiary graben, formed in metamorphic crystalline rocks, was subsequently filled with fluvial and lacustrine sediments (>1000 m thick) [Beaubien et al., 2004]. The Florina basin is flanked on the west side by a normal fault zone and metamorphic rocks intruded by granites, and on the east side by crystalline limestones, schists and gneisses. Moving eastward in the basin, sedimentary cover thins and changes from coarse clastics to sequences of sand, silt, clay, and lignite. Vertically stacked reservoirs of >99.5% CO_2 are located in limestone basement and overlying sandstone units, with the top of the upper reservoir located at only 300 m depth [Beaubien et al., 2004]. Sandstone reservoirs are capped by clayey sediments. CO_2 leakage at the surface in the Florina basin occurs as CO_2-rich springs throughout the area and, where basement limestones are exposed, as surface gas seeps. The Florina basin is seismically active, with earthquake magnitudes up to 5 on the Richter scale; the potential relationship between fluid migration and seismicity is being investigated [Beaubien et al., 2004].

2.3. INDUSTRIAL ANALOGUES

2.3.1. Introduction

Large-magnitude releases of gas associated with industrial processes have occurred relatively infrequently from geologic CO_2 reservoirs and natural gas storage facilities. Nonetheless, these events serve as important industrial analogues for the potential release of CO_2 from storage reservoirs due to human-related practices (e.g., well construction, injection and withdrawal practices). Here, we first describe large releases of CO_2 from geologic CO_2 reservoirs due to well blowouts. Each of these releases is also summarized with respect to their key characteristics and remedial measured applied in Table A.1 (Appendix). We then detail several cases of large releases of natural gas from storage facilities. While CH_4 is less dense and soluble than CO_2, and therefore will migrate in the subsurface and dissipate in the atmosphere more quickly than CO_2, important lessons can still be learned from natural gas releases and applied to geologic carbon sequestration projects.

2.3.2. Sheep Mountain, Colorado, USA

The Sheep Mountain CO_2 field is located in the Colorado Plateau area of southern Colorado. The CO_2 reservoir is located at 1000 to 1800 m depth in a northwest-trending anticlinal fold, bounded on the northeast side by a thrust fault [Allis et al., 2001]. The CO_2 reservoir units are the Cretaceous Dakota and Jurassic Entrada sandstones and are sealed by Cretaceous marine sediments capped by a laccolith [Allis et al., 2001]. The origin of the CO_2 is from thermal decomposition of limestones associated with magmatic intrusion [Caffee et al., 1999].

Production of the Sheep Mountain CO_2 field began in 1975 and has continued at about 2×10^9 m^3 yr^{-1}. The produced gas is 97% CO_2 and total reserves are estimated to be 7×10^{10} m^3 [Allis et al., 2001]. In March, 1982, a production well blew out of control during drilling, resulting in freely flowing CO_2 at the well head and leakage of CO_2 from ground fractures on the west slope of Little Sheep Mountain directly above the drill site [Lynch, 1983]. The “kill” operation was

complicated by the high CO_2 flow rate from the reservoir, which lifted the kill fluid (brine and mud) up the annulus. The well was brought under control in April, 1982 by the dynamic injection of drag-reduced brine followed by mud [Lynch, 1983].

2.3.3. Crystal and Woodside Geysers, Utah, USA

A number of well bores drilled for water or oil exploration discharge CO_2-rich groundwater along the Little Grand Wash and Salt Wash faults in the Paradox basin of Utah (see section 2.3.12). The most dramatic of these CO_2 leaks is Crystal Geyser, a cold-water geyser located on the eastern bank of the Green River in the footwall of the Little Grand Wash fault zone [Baer and Rigby, 1978] (Figure 2.19). Crystal Geyser erupts from the Glen Ruby #1-X oil exploration well that was drilled in 1935. The well was spudded into a 21.5 m thick travertine mound, drilled to a depth of 801 m, and then abandoned after oil was not found. Crystal Geyser currently erupts from the well bore to over 20 m high about every 12 hours. Because this is an artesian well, the CO_2-charged water rises in the well, the pressure decreases, and explosive degassing of dissolved CO_2 occurs. As the CO_2-charged waters continue to flow to the surface, the process is repeated.

Figure 2.19. Photo of an eruption of Crystal Geyser, UT.

Gouveia et al. [2005] measured atmospheric CO_2 concentrations on a grid 25 to 100 m away from Crystal Geyser, along with wind speed and direction. Based on Gaussian modeling of these data, CO_2 emission rate was estimated to be ~224 to 500 t d^{-1} during eruption events, and ~15 t d^{-1} during pre-eruptive events. They estimated the annual CO_2 emission rate from Crystal Geyser to be 12 kilotonnes. CO_2 concentrations were below human health and safety concerns, even within a few meters of the geyser.

Tenmile geyser is located near the northern extent of the Salt Wash faults. The geyser erupts infrequently to a height of several meters from an abandoned well drilled to a depth of 200m in the fault footwall (e.g., Shipton and others 2004). Other smaller geysers (e.g., the Woodside, Tumbleweed, and Chaffin Ranch geysers) also erupt occasionally from abandoned water and oil

exploration wells drilled in the northern Paradox basin. No health or safety effects related to the geysers are reported in the literature.

2.3.4. Florina basin, Greece

The Florina CO_2 field, located in the Florina basin (described in section 2.3.13), is the only commercial, naturally-sourced CO_2 producer in Greece. The field has been in production over the last ten years, with production ranging from 20,000 to 30,000 t yr^{-1} over the past three years [e,.g., Beaubien et al., 2004]. As summarized in NASCENT [2005], in 1990, the Department of Hydrogeology, IGME drilled an exploration well for mineral water to 559 m depth in the Florina basin. After the well was completed and the wellhead valve was closed, surface CO_2 leakage was observed 100 m from the well. The area of leakage moved toward the well, creating a ~25 m^2 hole around it, and allowing the drill rig platform to collapse into it. A small lake was formed in the hole and the area was fenced off to people and animals. A small pool was later built for people to immerse their feet in; however, when one person attempted to swim in the pool and died of CO_2 asphyxiation, it was closed by local authorities. In 2000, water was observed to still be flowing in the pool, while in 2003, the well and pool were dry, likely due to lowering of gas pressure in the reservoir and borehole collapse [NASCENT, 2005].

2.3.5. Torre Alfina Geothermal Field, Italy

The Torre Alfina geothermal field is located in northern Latium, central Italy. This field is water dominated, with a gas cap composed primarily of CO_2 overlying the reservoir. The cap rock on the reservoir consists of sequences of shales, marls, and limestones. In 1973, the first exploratory well (Alfina 1) was drilled through 20 m of volcanics and then the cap rock to a depth of 663 m, at which point it blew out, producing over 300 t h^{-1} of fluid, primarily gas [Ferrara and Stefani, 1978]. After releasing ~25,000 t of CO_2 to the atmosphere, the well was shut in. Numerous areas of surface CO_2 emissions then appeared around the well and were attributed to a lack of production casing and CO_2 migration along permeable pathways in the cap rock and overlying volcanics. Due to the potential danger to the rig technicians and local residents associated with high CO_2 emissions, the well was completely cemented. Three boreholes were also drilled in an effort to focus subsurface CO_2 flow to a few points and release the CO_2 at a height above the ground surface where the hazards associated with the gas would be reduced. However, this was only successful at one of the boreholes.

Ferrara and Stefani [1978] conducted a survey of atmospheric CO_2 concentrations associated with the surface CO_2 emissions within a 250-m diameter area around the Alfina 1 well. Over a 53-day survey period, they measured CO_2 concentrations of up to ~50%. The highest values were measured closest to the ground surface (10 cm height above ground), in topographic depressions, and during periods of low wind speed.

2.3.6. Hutchinson, Kansas, USA

The Yaggy natural gas storage facility is located seven miles northwest of the town of Hutchinson (population 40,000), located in central Kansas. The storage facility consists of 160 solution-mined salt caverns at 150 to 200 m depth. On the morning of January 17, 2001, a gas explosion occurred beneath two stores in downtown Hutchinson. Later that day, gas and water

geysers began erupting two miles to the east along the edge of Hutchinson, and continued to erupt over the next several days. One explosion beneath a trailer home killed two people.

To determine the gas migration pathway, 54 vent and observation wells were drilled in the Yaggy and Hutchinson area. Based on seismic profiling, cores, gas shows while drilling, and wireline logs, the leak apparently originated through a cracked gas well casing at 181 m depth (56 m above the top of the salt cavern), migrated to the shallow dolomitic horizon (128 m), then updip along the crest of a narrow, low-relief, northwesterly plunging anticline [Watney et al., 2003]. Pressure-induced parting along a pre-existing fracture system on the anticlinal crest likely occurred [Watney et al., 2003], allowing gas migration to the surface along abandoned brine wells. The source of the gas leak was stopped by plugging the damaged well, and the surface leaks were stopped by plugging the abandoned brine wells located using electromagnetic metal detectors.

2.3.7. Leroy Gas Storage Facility, Wyoming, USA

The Leroy gas storage facility in Wyoming consists of a confined sandstone and dolomite aquifer at 1000 m depth. A well casing here was installed in 1971 and failed due to corrosion in 1973 [Araktingi et al., 1984]. Gas then migrated horizontally to another well through a formation above the storage reservoir, vertically along the outside of the well casing, and bubbled out at the surface. In 1975 or 1976, gas again leaked from the storage site from one well casing and in 1978, bubbled out at the surface through a creek and pond near two wells. Gas bubbling in some areas occurred intermittently, ceasing when storage pressures were decreased, which was interpreted to indicate direct leakage from the reservoir to the surface. In other areas, bubbling was constant, which may have been due to storage in a secondary shallow trap [Araktingi et al., 1984].

The tracers reached the bubbling areas within 9 to 71 days following their injection into numerous wells. Based on tracer tests, pressure/inventory data, and computer modeling, it was determined that leakage from the storage reservoir only occurred when a threshold pressure was exceeded. The average annual leakage rate from 1976 to 1981 was ~3 % of the total gas stored, or 3×10^6 m^3 yr^{-1}. After 1981, gas leakage was controlled by limiting maximum injection pressures. The gas leak did not adversely affect operations at the gas storage project and no adverse health/safety effects were noted [Araktingi et al., 1984].

2.3.8. Kingfisher, OK, USA

The Edmundson Trust #1-33 well is located in southeast Kingfisher County, Oklahoma, about 14 miles southwest of the town of Kingfisher. The well was spudded in the Permian Flowerpot shale, which overlies the Hennesey Group (Cedar Hills sandstone, Hennesey shale, Garber sandstone, from top to bottom) [Miller, 2005]. The Hennesey group overlies the Wellington formation, which is composed of sandstone and several evaporite units. While drilling the Edmundson Trust #1-33 well, the Chesapeke Energy Corp. reported that they encountered a high-pressure gas pocket at about 9,400 feet below the surface and then gas escaping into the formation wall between 1,300 and 1,700 feet depth [Miller, 2005]. Several days later, on December 9, 2005, a hunter found natural gas geysers erupting along Winter Camp Creek. The geysers erupted in clusters, and defined a linear, 10-mile-long feature oriented perpendicular to

the regional strike of the bedding. It was hypothesized that the gas flowed along the well casing toward the surface, bypassing the Hennesey shale and escaping at the surface, where the Cedar Hills sandstone is exposed in creek beds [Miller, 2005]. Some unknown fracture system may also have controlled gas migration in the near surface, resulting in the observed distribution of surface gas features. Based on the isotopic compositions of gas samples collected from the well head and a geyser, the gases erupted at the surface likely originated from the high-pressure gas pocket at depth [Miller, 2005]. The Chesapeake Energy Corp. plugged the Edmundson Trust #1-33 well, and by January, 2006, the geysering was significantly reduced [http://www.kotv.com/main/home/stories.asp?whichpage=1&id=97416]. It was estimated that more than 45 million cubic feet of gas were released to the atmosphere [http://www.kotv.com/main/home/stories.asp?whichpage=1&id=97416].

3. GROUNDWATER QUALITY

3.1. INTRODUCTION

The leakage of CO_2 and related minor chemical constituents (e.g., SO_x, NO_x) that may be injected from geologic storage reservoirs has the potential to contaminate groundwater by acidification and subsequent reaction with host rocks along flow paths. The natural leakage of CO_2 (plus additional acid gases in some cases) from geologic reservoirs into groundwaters can serve as an analogue for acid gas release from storage reservoirs to better understand the potential risks to groundwater quality. Below, we briefly summarize the chemical composition of typical flue and fuel gas streams and the processes used to separate and capture highly concentrated CO_2. We then describe several natural analogues for the leakage of CO_2 into groundwaters, with emphasis on the resulting groundwater chemical compositions.

3.2. CHEMICAL COMPOSITION OF FLUE GAS STREAMS AND CO_2 SEPARATION

Table 3.1 [Mahasenan and Brown, 2004, and references therein] summarizes the chemical compositions by volume of flue (and fuel) gases from selected coal, fuel oil, natural gas, and gas turbine power plants. As shown, the major constituent (~71-75%) in flue gas streams is N_2, whereas CO_2 concentrations range from ~3 to 14%, resulting from the combustion of fossil fuel in air. Also present in significant concentrations are H_2O and O_2, while trace quantities of NO_x and SO_x can be present in the flue gas stream of coal and fuel oil power plants. The composition of the fuel gas stream from the integrated gasification combined-cycle (IGCC) power plant is comparatively high in CO_2 (~39%) and H_2 (~57%), and low in N_2, H_2O, and O_2.

Table 3.1. Chemical composition (volume %) of flue and fuel gas streams.

Plant type	Stream	N_2	H_2O	O_2	CO	CO_2	CH_4	H_2	Ar	NO_x	SO_x
Coal[1]	Flue	74.0	8.0	3.0		14.0			1.0	0.0	0.1
Coal[2]	Flue	71.4	10.8	4.3		12.6			0.9	0.0	0.0
Fuel oil[3]	Flue	73.0	13.0	3.0		11.0				trace	trace
Natural gas[4]	Flue	71.0	17.0	3.0		9.0				0.0	0.0

Natural gas[5]	Flue	70.9	17.3	2.4		8.6			0.9		
Gas turbine[1]	Flue	75.7	7.8	13.0		3.5					
Gas turbine[2]	Flue	75.0	6.9	13.8		3.4			0.9	0.0	
Gas turbine[4]	Flue	74.4	8.3	12.6	0.0	3.8	0.0	0.0	0.9	0.0	0.0
Coal IGCC[5]	Fuel	0.7	1.7	0.0	1.7	38.6	0.1	56.7	0.6	0.0	0.0

[1]IEA, 1993
[2]Electric Power Research Institute, 2000
[3]Suda et al., 1992
[4]Ijima, 1998
[5]National Energy Technology Laboratory, 2000

Several methods can be applied to separate flue gas and capture highly concentrated (typically >99%) CO_2. One method is based on chemical absorption. In this process, flue gas is bubbled through a liquid solvent (e.g., aqueous amine solution) in a packed absorber column and the CO_2 is removed by the formation of a chemically bonded compound. The CO_2 is then stripped from the solvent when the solvent is passed through counterflowing steam, and a highly concentrated CO_2 stream is left when the steam is condensed. This method is most successful when applied to flue gas streams with low CO_2 partial pressure and is intolerant of SO_x, NO_x, fly ash, and high flue gas temperatures. A second method is based on the physical absorption of CO_2 by solvents (e.g., Selexol, hindered amines, and hot potassium carbonate). As CO_2 capture is directly proportional to the CO_2 partial pressure in the flue gas, this method is most applicable to high-pressure gas streams. Hybrid absorption processes combine chemical and physical absorption methods to capture CO_2 from gas streams that have variable CO_2 concentrations and pressures. Other separation and capture methods include membrane-absorption and oxy-fuel combustion processes. Further details about CO_2 separation and capture methods can be found in, e.g., Herzog et al. [1997], Dave et al. [2001], and Mahasenan and Brown [2004].

3.3. NATURAL ANALOGUES

3.3.1. San Vittorino, Italy

The San Vittorino plain, located 100 km northeast of Rome in central Italy, is a sparsely populated intramontane basin that is used primarily for agriculture. Carbonate rocks are prevalent in the region (e.g., bedrock limestones and surface travertines). Numerous CO_2-rich mineral springs, gas vents, and sinkholes, many of which pose hazards to local infrastructure, are located throughout the plain, and are believed to be associated with migration of CO_2 from depth along major faults in the area. In an effort to understand the influence of this CO_2 leakage on groundwater chemistry and sinkhole formation, NASCENT [2005] conducted soil gas, bubble gas, dissolved gas, and groundwater geochemistry surveys throughout the plain. They found that anomalously high soil gas concentrations (up to 70% CO_2, 80 ppm He, and 2% CH_4) were closely correlated with the locations of sinkholes. Gas bubbles in springs, sinkholes, and wells had concentrations of CO_2 from 36 to 85%, CH_4 from 150 to 2100 mg L^{-1}, He from 6 to 400 mg

L^{-1}, and N_2 from 7 to 60%. H_2S was also present, but unquantified. Dissolved gases had CO_2 concentrations from <0.2 to 0.8 L gas per L water at standard pressure and temperature. The highest CO_2 concentrations were close to the solubility limit of CO_2 in water. Chemical analysis of waters collected from springs, wells, and sinkholes indicated that most are classified as Ca-HCO_3 waters, while a few were classified as Ca-Mg-HCO_3 waters. The total dissolved constituents varied widely between samples, with Total Dissolved Solids ranging from 330 to 1843 mg L^{-1} and hardness ranging from 307 to 1843 mg L^{-1} as $CaCO_3$. The concentrations of major elements were well correlated in samples. Concentrations ranged from 89-550 mg L^{-1} for Ca, 17 to 97 mg L^{-1} for Mg, 10 to 795 mg L^{-1} for SO_4, 43 to 1945 mg L^{-1} for B, and 230 to 2900 mg L^{-1} for Sr. Some waters were also enriched in Mn, Al, Zr, Pd, and Rb. Samples with the highest concentrations of dissolved constituents were located in the north-central part of the plain and also had the highest CO_2 concentrations in dissolved and bubble gases. The leakage of CO_2 (and H_2S) typically resulted in a 5 to 10 times increase in most major and trace elements in springs. Despite elevated concentrations of dissolved chemical constituents in groundwaters, most waters were potable.

Correlations between dissolved chemical constituents in waters were interpreted to reflect the dissolution of carbonate rocks along flowpaths of groundwaters that have become acidified by CO_2 and H_2S rising along high permeability pathways in fault zones. The formation of sinkholes was found to be closely associated with groundwaters with anomalously high dissolved chemical constituents. These features were likely formed by the dissolution of fine-grained rocks by acidified groundwaters and collapse triggered by earthquakes. NASCENT [2005] developed and deployed a continuous groundwater chemistry monitoring station in the San Vittorino plain, designed to detect anomalous changes that may serve as precursors to sinkhole formation.

3.3.2. Florina Basin, Greece

Two aquifers are present in the Florina basin (see Section 2.3.13). One is a confined aquifer in clastic sedimentary rocks capped by silts and clays that extends throughout most of the basin and hosts the CO_2 reservoir. The second is an unconfined aquifer hosted in karstic carbonates on the eastern and southern margins of the basin. To evaluate the effects of CO_2 leakage from depth on groundwater quality in the Florina basin, Beaubien et al. [2004] conducted an investigation of the chemistry of waters from wells and springs throughout the basin. They analyzed major element concentrations in 132 samples and trace element concentrations in 17 of these samples and found that total dissolved solids ranged from 150 to 4230 mg L^{-1} and hardness ranged from 70 to 1950 mg L^{-1} as $CaCO_3$. Waters collected from shallow wells and springs were Ca-HCO_3 type, while those collected from deep boreholes were Mg-HCO_3 type. Most water samples were potable. However, samples collected close to the CO_2 field had higher total dissolved chemical constituents and hardness, and consequently were of poorer drinking water quality. Beaubien et al. [2004] interpreted the spatial trends in the chemical compositions of groundwaters to reflect interaction of CO_2-rich groundwaters with host rocks along flow paths.

3.3.3. Albani Hills, Italy

Three main hydrogeologic units have been identified in the Albani Hill region (see Section 2.3.4) [Boni, et al., 1995]. From depth to the surface, these include: (1) a calcareous-siliceous-marly basal complex constituting a multi-layered aquifer hosted in fractured carbonates interbedded

with confining clay layers, (2) a clayey-marly intermediate complex that acts as a groundwater flow boundary due to its low permeability, and (3) the Albani Hills volcanic complex which displays wide variation in permeability and acts as a multi-layered aquifer with radial groundwater flow. Chiodini and Frondini [2001] conducted a geochemical study of groundwaters collected from 293 wells and 63 springs in the region (Figure 3.1) and found elevated CO_2 partial pressures (average = 0.2 bar), indicating a high CO_2 leakage rate into the regional aquifers. HCO_3 is the major anion in most waters, while only a few samples are characterized by high Cl and SO_4 concentrations. The SO_4-rich waters in the northern part of the study area are speculated to be associated with influx of deep sulfur-rich gases into shallow groundwaters, while the Cl-rich waters are located on the coastal plain and are associated with fossil seawater. The relative concentrations of cations (e.g., Na/K ratios, Figure 3.1) in waters reflect interaction of CO_2-rich groundwaters with host rocks. In particular, many samples have high HCO_3, Ca, and Mg contents, which can be explained by the influx of CO_2-rich fluids from depth and subsequent interaction with sedimentary rocks.

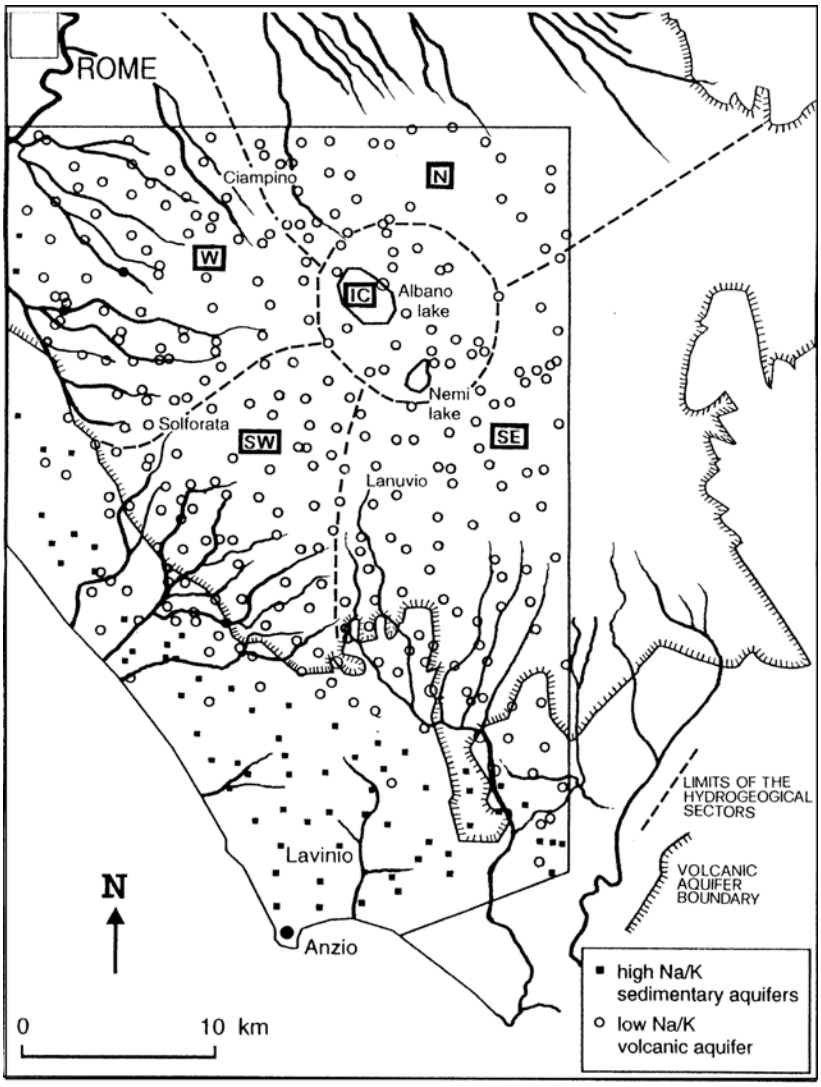

Figure 3.1. Map of the Albani Hills region showing major drainage basins and locations of water samples from Chiodini and Frondini [2001].

3.3.4. Central Italy

Throughout Tyrrhenian Central Italy, widespread non-volcanic CO_2 degassing (possibly originating from a crustally-contaminated mantle or a mixture of magmatic and crustal components) occurs from vent and diffuse soil gas emissions and from CO_2-enriched groundwaters [Chiodini et al., 1999]. From the Tyrrhenian Sea to the Apennine Mountains, buried structural highs act as gas traps. Widespread CO_2 leakage occurs at the surface throughout the region in the form of diffuse and vent gas emissions or by dissolution in groundwaters and subsequent release at surface springs. Chiodini et al. [1999, 2000] conducted geochemical investigations of regional aquifers and found elevated CO_2 partial pressure values in spring discharges (e.g., 2.51×10^{-3} to 8.14×10^{-1} bar, average 3.12×10^{-1} bar). They also found that in geographic regions characterized by thick regional carbonate-evaporite aquifers, most or part of the deeply derived gas is dissolved by the aquifers, whereas in regions characterized by small aquifers, these aquifers cannot dissolve a large quantity of the CO_2 and extensive vent and soil CO_2 emissions occur at the surface. Chiodini et al. [2000] used mass balance equations coupled with carbon isotopic analyses and hydrologic data to estimate fluxes of deeply derived CO_2 of up to 0.29 g $m^{-2}d^{-1}$ into the aquifers. For waters with high CO_2 partial pressures, the CO_2 flux lost to the atmosphere is of the same order of magnitude as the influx of deep CO_2**.**

Based on the analysis of major dissolved chemical constituents in 52 springs, 65% were classified as Ca(Mg)-HCO_3 in composition, 10% as Ca-Mg-SO_4 in composition, 10% as Na-Cl in composition, and the remaining as intermediate in composition [Chiodini et al., 2000]. A major process controlling the chemical composition of most groundwaters was the dissolution of calcite, while the dissolution of gypsum or halite was important in the springs of a few aquifers. Total dissolved inorganic carbon concentrations in springs ranged from 0.00244 to 0.05080 mol kg^{-1}.

3.3.5. Mammoth Mountain, California, USA

Mammoth Mountain in eastern California (see Section 2.3.2) has numerous CO_2-rich cold springs located on its lower flanks, primarily associated with leakage from the high-pressure gas reservoir beneath the volcano [Evans et al., 2002]. Evans et al. [2002] conducted a geochemical study of these springs to quantify the magmatic carbon discharge in cold groundwaters. Based on measured spring flow rates and concentrations and isotopic compositions of dissolved inorganic carbon in spring discharges, they found that Mammoth discharges 2×10^4 t yr^{-1} of deeply derived carbon (as CO_2); this discharge varies seasonally from 30 to 90 t d^{-1}. While most springs contain high concentrations of dissolved CO_2, they are otherwise dilute, with specific conductance ranging from 100 to 300 μS cm^{-1}.

3.3.6. Paradox Basin, Utah, USA

A number of natural springs and well bores discharge CO_2-rich groundwater along the Little Grand Wash and Salt Wash faults in the Paradox basin of Utah (see sections 2.3.12 and 2.4.3). Samples collected from springs along the Little Grand Wash and Salt Wash faults and from Crystal Geyser were analyzed to determine the contents of major dissolved chemical constituents in groundwaters [Shipton et al., 2004]. Concentrations (in mmol L^{-1}) were as follows: 2.37-20.83 for Ca, 7.86 to 9.30 for Mg, 167.82-236.38 for Na, 7.62 to 10.44 for K, 0.00 to 0.14 for Fe,

0.00 to 0.02 for Mn, 0.01 to 0.16 for Sr, 46.40-75.70 for HCO_3, 91.15-204.52 for Cl, and 24.33-30.81 for SO_4. Waters were high in total dissolved solids, which ranged from 13555 to 21188 mg L^{-1}. Shipton et al. [2004] determined that the chemical compositions of groundwaters were primarily controlled by the dissolution of calcite and evaporites along groundwater flow paths.

4. CONCLUSIONS

Large-magnitude releases of CO_2 have occurred naturally from geologic reservoirs in numerous volcanic, geothermal, and sedimentary basin settings. In addition, CO_2 and natural gas have been released from geologic CO_2 reservoirs and natural gas storage facilities, respectively, due to influences such as well defects and injection/withdrawal processes. These systems serve as natural and industrial analogues for the potential release of CO_2 from geologic storage reservoirs and provide important information about the key features, events, and processes that are associated with releases, as well as the health, safety, and environmental consequences of releases and mitigation efforts that can be applied. Based on an analysis of a broad range of natural and industrial analogues for CO_2 leakage, the following conclusions can be drawn, and lessons can be learned for risk assessment associated with geologic carbon storage:

(1) Carbon dioxide can both accumulate beneath, and be released from, primary and secondary reservoirs with capping units located at a wide range of depths. Both primary and secondary reservoir entrapments for CO_2 should therefore be well characterized at storage sites.

(2) Many natural releases of CO_2 have been correlated with a specific event that has triggered the release, such as magmatic or seismic activity. The potential for processes that could cause geomechanical damage to sealing cap rocks and trigger the release of CO_2 from a storage reservoir should be evaluated.

(3) Unsealed fault and fracture zones can act as fast and direct conduits for CO_2 flow from depth to the surface. Risk assessment should emphasize determining the potential for and nature of CO_2 migration along these structures.

(4) Wells that are structurally unsound have the potential to release large quantities of CO_2 rapidly to the atmosphere. Risk assessment should therefore be focused on the potential for both active and abandoned wells at storage sites to transport CO_2 to the surface, particularly in depleted oil or gas reservoir systems, where wells are abundant.

(5) The style of CO_2 release at the surface varies widely between and within different leakage sites. In rare circumstances, the release of CO_2 can be a self-enhancing and/or eruptive process; this possibility should be assessed in the case of CO_2 leakage from storage reservoirs.

(6) The hazard to human health was small in most cases of large surface releases of CO_2. This could be due to implementation of public education and CO_2 monitoring programs; these programs should therefore be employed to minimize potential health, safety, and environmental effects associated with CO_2 leakage.

(7) While changes in groundwater chemistry can be related to CO_2 leakage due to acidification and interaction with host rocks along flow paths, waters remained potable in most cases. Groundwaters should be monitored for changes in chemistry that could result from leakage from CO_2 leakage from storage sites.

REFERENCES

Aeschbach-Hertig, W., R. Kipfer, M. Hofer, D.M. Imboden, R. Wieler, and P. Signer, Quantification of gas fluxes from the subcontinental mantle: The example of Laacher See, a maar lake in Germany, *Geochim. Cosmochim. Acta, 60*, 31-41, 1996.

Allard, P., D. Dajlevic, and C. Delarue, Origin of carbon dioxide from the 1979 Dieng eruption, Indonesia: Implications for the origin of the 1986 Nyos catastrophe, *J. Volcanol. Geotherm. Res., 39*, 195-206, 1989.

Allard, P., A. Maiorani, D. Tedesco, G. Cortecci, and B. Turi, Isotopic study of the origin of sulfur and carbon in Solfatara fumaroles, Campi Flegrei caldera, J. Volcanol. Geotherm. Res., 48, 139-159, 1991.

Allis, R., T. Chidsey, W. Gwynn, C. Morgan, S. White, M. Adams, J. Moore, Natural CO_2 reservoirs on the Colorado Plateau and southern Rocky Mountains: Candidates for CO_2 sequestration, in *Proceedings of the First National Conference on Carbon Sequestration*, National Energy Technology Laboratory, U.S. Department of Energy, Washington, D.C., May 14-17, 2001.

Allis, R., D. Bergfeld, J. Moore, K. McClure, C. Morgan, T. Chidsey, J. Heath, and B. McPherson, Implications of results from CO_2 flux surveys over known CO_2 systems for long-term monitoring, *Fourth Annual Conference on Carbon Capture and Sequestration DOE/NETL*, May 2-5, 2005.

Annunziatellis, A., G. Ciotoli, S. Lombardi, and F. Nolasco, Short and long term gas hazard: the release of toxic gases in the Alban Hills volcanic area (central Italy), *J. Geochem. Explor*., 77, 93-108, 2003.

Annuziatellis, A., G. Ciotoli, E. Pettinelli, S.E. Beaubien, Geochemical and geophysical characterization of an active gas vent near the village of Latera, central Italy, *GHGT7*, Vancouver, Sept. 5-8, 2004.

Araktingi, R.E., M.E. Benefield, Z. Bessenyei, K.H. Coats, and M.R. Tek, Leroy gas storage facility, Unita County, Wyoming: A case history of attempted gas-migration control, *J. Petrol. Tech., 36*, 132-140, 1984.

Astorri, F., S.E. Beaubien, G. Ciotoli, and S. Lombardi, An assessment of gas emanation hazard using a geographic informations system and geostatistics, *Health Phys., 82,* 358-366, 2002.

Baer, J.L. and J.K. Rigby, Geology of the Crystal Geyser and the environmental implications of its effluent, Grand County, Utah, *Utah Geology, 5*, 125-130, 1978.

Bailey, R.A., Geologic Map of the Long Valley Caldera, Mono-Inyo Craters Volcanic Chain, Eastern California, *U.S. Geol. Surv. Map I-1933*, 1989.

Bailey, R.A., G.D. Dalrymple, and M.A. Lanphere, Volcanism, structure, and geochronology of Long Valley caldera, Mono County, California, *J. Geophys. Res., 81*, 725-744, 1976.

Barberi , F., G. Corrado, F. Innocenti, G. Luongo, Phlegraean Fields 1982-1984: Brief chronicle of a volcano emaergency in a densely populated area, *Bull. Volcanol., 47,* 175-185, 1984.

Baxter, P.J. and M. Kapila, Acute health impact of the gas release at Lake Nyos, Cameroon, *J. Volcanol. Geotherm. Res., 39*, 265-275, 1989.

Beaubien, S.E., G. Ciotoli, and S. Lombardi, Carbon dioxide and radon gas hazard in the Alban Hills area (central Italy), *J. Volcanol. Geotherm. Res*., 123, 63-80, 2003.

Beaubien, S.E., S. Lombardi, G. Ciotoli, A. Annunziatellis, G. Hatziyannis, A. Metaxas, and J.M. Pearce, Potential Hazards of CO_2 leakage in storage systems – learning from natural systems, *GHGT7*, Vancouver, Sept. 5-8, 2004.

Benson, S.M., R. Hepple, J. Apps, C.-F. Tsang, and M. Lippmann, Lessons learned from natural and industrial analogues for storage of carbon dioxide in deep geological formations, *Lawrence Berkeley National Laboratory Report LBNL-51170*, 2002.

Bergfeld, D., Carbon dioxide flux and carbon reservoirs in the Geysers-Clear lake geothermal region of northern California, *Eos, Trasactions, AGU Fall Meet. Suppl.* 1997.

Bergfeld, D., F. Goff, and C.J. Janik, Carbon isotope systematics and CO_2 sources in The Geysers-Clear Lake region, northern California, USA, *Geothermics, 30*, 303-331, 2001.

Boni, C., P. Bono, S. Lombardi, L. Mastrorillo, and C. Percopo, Hydrogeology, fluid geochemistry, and thermalism, In: Triglia, R. (Ed.), *The Volcano of the Alban Hills, Rome*, pp. 221-242, 1995.

Caffee, M.W., G. B. Hudson, C. Velsko, G. R. Huss, E. C. Alexander Jr., and A. R. Chivas, Primordial noble gases from Earth's mantle: identification of a primitive volatile component, *Science, 285*, 2115-2118, 1999.

Cavarretta, G., G. Gianelli, G. Scandiffo, and F. Tecce, Evolution of the Latera geothermal system II: metamorphic, hydrothermal mineral assemblages and fluid chemistry, *J. Volcanol. Geotherm. Res., 26*, 337-364, 1985.

Chiodini, G. and F. Frondini, Carbon dioxide degassing from the Albani Hills volcanic region, Central Italy, *Chem. Geol., 177*, 67-83, 2001.

Chiodini, G., F. Frondini, D.M. Kerrick, J. Rogie, F. parello, L. Peruzzi, and A.R. Zanzari, Quantification of deep CO_2 fluxes from Central Italy. Examples of carbon balance for regional aquifers and of soil diffuse degassing, *Chem. Geol., 159*, 205-222, 1999.

Chiodini, G., F. Frondini, C, Cardellini, F. Parello, and L. Peruzzi, Rate of diffuse carbon dioxide Earth degassing estimated from carbon balance of regional aquifers: The case of the central Apennine, Italy, *J. Geophys. Res., 105*, 8423-8424, 2000.

Chiodini, G., F. Frondini, C. Cardellini, D. Granieri, L. Marini, and G. Ventura, CO_2 degassing and energy release at Solfatara volcano, Campi Flegrei, Italy, *J. Geophys. Res., 106,* 16,213-16,221, 2001.

Choet, B., New methods and future trends in seismological volcano monitoring, In: Scarpa, R. and Tilling, R.I. (Eds.), *Monitoring and Mitigation of Volcanic Hazards*, Springer-Verlag, Berlin, 23-97, 1996.

Cioni, R., E. Corazza, and L. marini, The gas/steam ratio as an indicator of heat transfer at Solfatara fumaroles, Phlegraean Fields (Italy), *Bull. Volcanol., 47*, 295-302, 1984.

Cook, A.C., L.J. Hainsworth, M.L. Sorey, W.C. Evans, and J.R. Southon, Radiocarbon studies of plant leaves and tree rings from Mammoth Mountain, CA: a long-term record of magmatic CO_2 release, *Chem. Geol., 177*, 117-131, 2001.

Corrado, G., Guerra, L., Lo Bascio, A., Luongo, G. and Rampoldi, R., Inflation and microearthquake activity of Phlegraean Fields, Italy. *Bull. Volcanol., 40*, 169-185, 1977.

Dave, N., C. Fookes, and C. Walters, Assessment of novel technologies for CO_2 capture and separation, *Proceedings of the Eighteenth Annual International Pittsburgh Coal Conference*, Newcastle, 2001.

De Rita, D., C. Faccenna, R. Funicello, and C. Rosa, Stratigraphy and volcano-tectonics, In: R. Triglia (Ed.), *The volcano of the Alban Hills, Rome*, 167-192, 1995.

Dickinson, W.R. and W.S. Snyder, Geometry of subducted slabs related to San Andreas transform, *J. Geol., 87*, 609-627, 1979.

Donnolly-Nolan, J.M., M.G. Burns, F.E. Goff, E.K. Peters, and J.M. Thompson, The Geysers-Clear Lake area, California: thermal waters, mineralization, volocanism, and geothermal potential, *Econ. Geol., 88*, 301-316, 1993.

Electric Power Research Institute, *Evaluation of Innovative Fossil Fuel Power Plants with CO_2 Removal*, 2000.

Evans, W.C., L.D. White, M.L. Tuttle, G.W. Kling, G. Tanyileke, and R.L. Michel, Six years of change at Lake Nyos, Cameroon, yield clues to the past and cautions for the future, *Geochem. J., 28*, 139-162, 1994.

Evans, W.C., M.L. Sorey, A.C. Cook, B.M. Kennedy, D.L. Shuster, E.M. Colvard, L.D. White, and M. A. Huebner, Tracing and quantifying magmatic carbon discharge in cold groundwaters: lessons learned from Mammoth Mountain, USA, *J. Volcanol. Geotherm. Res., 114*, 291-312, 2002.

Farrar, C.D., M.L. Sorey, W.C. Evans, J.F. Howle, B.D. Kerr, B.M. Kennedy, C.-Y. King, and J.R. Southon, Forest-killing diffuse CO_2 emission at Mammoth Mountain as a sign of magmatic unrest, implications for flux measurements, *Nature, 376*, 675-678, 1995.

Farrar, C.D., J.M. Neil, and J.F. Howle, magmatic carbon dioxide emissions at Mammoth Mountain, California. U.S. Geological Survey, *Water Resources Investigations Report 98-4217*, 1999.

Ferrara, G.C. and G. Stefani, CO_2 distribution in the atmosphere and noise survey after blow-out in Alfina 1 well, northern Latium, Italy, *Geothermics, 6*, 163-174, 1977.

Fink, J.H., The geometry of silicic dikes beneath the Inyo domes, California, *J. Geophys. Res., 90*, 11,127-11,133, 1985.

Foulger, G.R., B.R. Julian, A.M. Pitt, and D.P. Hill, Seismic monitoring and activity increase is California caldera, *Eos, Trans.-AGU, 79*, 357-363, 1998.

Foulger, G.R., B.R. Julian, D.P. Hill, A.M. Pitt, P.E. Malin, and E. Shalev, Non-double-couple microearthquakes at Long Valley caldera, California, provide evidence for hydraulic fracturing. *J. Volcanol. Geotherm. Res., 132*, 45–71, 2004.

Freeth, S.J. and R.L.F. Kay, The Lake Nyos gas disaster, *Nature, 325*, 104-105, 1987.

Gerlach, T.M., M.P. Doukas, K.A. McGee, R. Kessler, Aiborne detection of diffuse carbon dioxide emissions at Mammoth Mountain, *Geophys. Res. Lett., 26*, 3661-3664, 1999.

Gerlach, T.M., M.P. Duukas, K.A. McGee, and R. Kessler, Soil efflux and total emission rates of magmatic CO_2 at the Horseshoe lake tree kill, Mammoth Mountain, California, 1995-1999, *Chem. Geol., 177*, 101-116, 2001.

Giggenbach, W.F., Water and gas chemistry of Lake Nyos and its bearing on the eruptive process, *J. Volcanol. Geotherm. Res. 42*, 337-362, 1990.

Giggenbach, W.F., Y. Sano, and H.U. Schminke, CO_2-rich gases from Lakes Nyos and Monoun, Cameroon; Laacher See, Germany; Dieng, Indonesia, and Mt. Gambier, Australia – variations on a common theme, *J. Volcanol. Geotherm. Res*., 45, 311-323, 1991.

Goff, F., A.I. Adams, P.E. Trujillo, D. Counce, J. Mansfield, Geochemistry of thermal/mineral waters in the Clear Lake region, California, and implications for hot dry rock geothermal development, *Los Alamos National Laboratory Report LA 12510-HDR*, 1993a.

Goff, F., B.M. Kennedy, A.I. Adams, P.E. Trujillo, and D. Counce, Hydrogeochemical evaluation of conventional and hot dry rock geothermal resource potential in the Clear Lake region, California, *Geotherm. Resour. Council Trans., 17*, 335-342, 1993b.

Goff , F.E., C.J. Janik, and J.A. Stimac, Sulfur bank mine, California: an example of a magmatic rather than metamorphic hydrothermal system?, *Proceedings of the World Geothermal Congress, Florence, Italy, 2*, 1105-1110, 1995.

Gouveia, F.J., M.R. Johnson, R.N. Leif, and S.J. Friedmann, Aerometric measurement and modeling of the mass of CO_2 emissions from Crystal Geyser, Utah, *Lawrence Livermore National Laboratory Report UCRL-TR-211870*, 2005.

Griesshaber, E., R.K. O'Nions, and E.R. Oxburgh, Helium and carbon isotope systematics in crustal fluids from the Eifel, the Rhine Graben, and Black Forest, F.R.G., *Chem. Geol., 99*, 213-235, 1992.

Halbwachs, M., J.-C. Sabroux, J. Grangeon, G. Kayser, J.-C. Tochon-Danguy, A. Felix, J.-C. Beard, A. Villenvielle, G. Vitter, P. Richon, A. Wuest, and J. Hell, Degassing the "Killer Lakes" Nyos and Monoun, Cameroon, *Eos, Trans., AGU, 85(30)*, 2004.

Heath, J.E., Hydrogeochemical characterization of leaking carbon dioxide-charged fault zones in east-central Utah, *MS Thesis, Utah State University*, 2004.

Herzog, H.J., E.M. Drake, and E.E. Adams, CO_2 capture, reuse, and storage technologies for mitigating global climate change – a "White Paper", *DOE Order No. DE-AF22-96PC01257*, 1997.

Hildreth, W., Volcanological perspectives on Long Valley, Mammoth Mountain, and Mono Craters: several contiguous but discrete systems, *J. Volcanol. Geotherm. Res., 136*, 169-198, 2004.

Hill, D.P., Temperatures at the base of the seismogenic crust beneath Long Valley Caldera, California, and the Phlegrean Fields caldera, Italy. In: Johnson, R.W. Mahood, G.A., and Scarpa, R. (eds.), *Volcanic Seismology*, Springer-Verlag, New York, pp. 432-461, 1992.

Hill, D.P., Earthquakes and carbon dioxide beneath Mammoth Mountain, California, *Seis. Res. Lett.*, 67, 8-15, 1996.

Hill, D.P. and S. Prejean, Magmatic unrest beneath Mammoth Mountain, California, *J. Volcanol. Geotherm. Res., 146*, 257-283, 2005.

Hill, D.P., R.A. Bailey, and A.S. Ryall, Active tectonic and magmatic processes beneath Long Valley caldera, eastern California: An overview, *J. Geophys. Res., 90*, 11,111-11,150, 1985.

Hill, D. P., W. L. Ellsworth, M. J. S. Johnston, J. O. Langbein, D. H. Oppenheimer, A. M. Pitt, P. A. Reasenberg, M. L. Sorey, and S. R. McNutt, The 1989 earthquake swarm beneath Mammoth Mountain, California: An initial look at the 4 May through 30 September activity, *Bull. Seismol. Soc. Am., 80*, 325–339, 1990.

Hill, D.P., P. Dawson, M.J.S. Johnston, A.M. Pitt, G. Biasi, and K. Smith, Very-long-period volcanic earthquakes beneath Mammoth Mountain, California, *Geophys. Res. Lett., 29*, 1370, 2002.

Hill, P.M., Possible asphyxiation from carbon dioxide of a cross-country skier in eastern California: A deadly volcanic hazard, *Wilderness and Environmental Medicine, 11,* 192-195, 2000.

Ijima, M., A feasible new flue gas CO_2 recovery technology for enhanced oil recovery, *SPE-39686, SPE/DOE Improved Oil Recovery Symposium*, Tulsa, Oklahoma, 1998.

International Energy Agency, *Greenhouse gas Emissions from Power Stations*, IEA Greenhouse Gas R & D Programme, IEA, Paris, 1993.

International Energy Agency, *Carbon Dioxide Utilization*, IEA Greenhouse Gas R & D Programme, IEA, Paris, 1997.

Johnson, C.M. and J.R. O'Neil, Triple junction magmatism: a geochemical study of Neogene volcanic rocks in western California, *Earth Planet. Sci. Lett., 71*, 241-262, 1984.

Langbein, J.O., D.P. Hill, T.N. Parker, and S.K. Wilkinson, An episode of reinflation of the Long Valley Caldera, eastern California: 1989–1991. *J. Geophys. Res., 98*, 15851–15870, 1993.

Langbein, J.O., D. Dzurisin, G. Marshall, R. Stein, and J. Rundle, Shallow and peripheral volcanic sources of inflation revealed by modeling two-color geodimeter and leveling data from Long Valley Caldera, California, 1988–1992. *J. Geophys. Res. 100*, 12487–12496, 1995.

LeGuern, F., H. Tazieff, R. Faive Pierret, Witness accounts of the catastrophic event of August 1986 at Lake Nyos (Cameroon), *J. Volcanol. Geotherm. Res., 51*, 171-184, 1992.

Locardi, E., G. Lombardi, R. Funicello, and M. Parotto, The main volcanic groups of Latium (Italy): relations between structural evolution and petrogenesis, *Geol. Romana, 17*, 279-300, 1975.

Lynch, R., E. McBride, T. Perkins, and M. Wiley, Dynamic kill of an uncontrolled CO_2 well, *Society of Petroleum Engineers, IADC-SPE 11378*, 1983.

Mahasenan and Brown, Beyond the big picture: characterization of CO_2-laden streams and implications for capture technologies, *Proceedings of the 7th International Conference on Greenhouse gas Control Technologies, GHGT-7,* Vancouver, Canada, 2004.

Martini, M., Thermal activity and ground deformation at Phlegraean Fields, Italy: precursor of eruptions or fluctuations of quiescent volcanism? A contribution to geochemical studies, *J. Geophys. Res., 91*, 12,255-12,260, 1986.

McGee, K.A. and T.M. Gerlach, Annual cycle of magmatic CO_2 in a tree kill soil at Mammoth Mountain: implications for soil acidification, *Geology, 26*, 463-466, 1998.

McGee, K.A., T.M. Gerlach, R. Kessler, M.P. Doukas, Geochemical evidence for a magmatic CO_2 degassing event at Mammoth Mountain, California, September-December 1997, *J. Geophys. Res., 105,* 8447-8456, 2000.

McLaughlin, R.J., Tectonic setting of pre-Tertiary rocks and its relation to geothermal resources in the Geysers-Clear Lake area, In: McLaughlin, R.J., Donnoly-Nolan, J.M. (Eds.), Research in The Geysers-Clear Lake Geothermal Area, Northern California, *U.S. Geol. Surv. Prof. Paper 1141*, 1981.

Miller, C.D., Holocene eruptions at the Inyo Craters volcanic chain, California: Implications for possible eruptions in Long Valley caldera, *Geology, 13*, 14-17, 1985.

Miller, G., The gas geysers near Kingfisher, Oklahoma, Petroleum Technology Transfer Council Regional Update, South Midcontinent Region, Fourth Publication, 2005.

Modjo, S., Volcanic activity, Dieng Volcanic Complex, *SEAN Bull., 4*, 4-7, 1979.

NASCENT, Natural analogues for the geological storage of CO_2, *NASCENT Report 2005/6 March*, 2005.

NEA/OECD, Features, events, and processes (FEPs) for geologic disposal of radioactive waste – an international database, *NEA-OECD Report NEA 02549, Nuclear Energy Agency – Organization for Economic Cooperation and Development*, 2000.

National Energy Technology Laboratory, Texaco Gasifier IGCC Base Cases, *PED-IGCC-98-001*, July, 1998 (latest revision June 2000).

Newhall, C.G. and D. Dzurisin, Historical Unrest at Large Calderas of the World, *U.S.G.S. Bull. 1855*, 1988.

Orsi, G., De Vita, S. and di Vito, M., The restless, resurgent Campi Flegrei nested caldera (Italy): constraints on its evolution and configuration. *J. Volcanol. Geotherm. Res., 74*, 179-214, 1996.

Pitt, A.M. and D.P. Hill, Long-period earthquakes in the Long Vallay Caldera region, eastern California, Geophys. Res. Lett., 21, 1679-1682, 1994.

Pitt, A.M., D.P. Hill, S.W. Walter, and M.J.S. Johnston, Midcrustal, long-period earthquakes beneath northern California volcanic areas, *Seis. Res. Lett., 73*, 144-152, 2002.

Prejean, S., A. Stork, W. Ellsworth, D. Hill, and B. Julian, High precision earthquake locations reveal seismogenic structures within Mammoth Mountain, California. *Geophys. Res. Lett. 30*, 2247, 2003.

The Press Democrat, Death linked to mineral pool, October, 10, 2000.

Quattrocchi, F. and M. Calcara, Emanazioni gassose nell' area de Ciampino (2/11/95) ed evento sismico dei Colli Albani (3/11/95), *ING internal report*, 1995.

Rahn, T.A., J.E. Fessenden, and M. Walhen, Flux chamber measurements of anomalous CO_2 emission from the flanks of Mammoth Mountain, California, *Geophys. Res. Lett., 23,* 1861-1864, 1996.

Reichle, D., et al., *Carbon Sequestration Research and Development*, DOE/SC/FE-1 U.S. Department of Energy, Washington, DC, 1999.

Rogie, J.D., D.M. Kerrick, M.L. Sorey, G. Chiodini, and D.L. Galloway, Dynamics of carbon dioxide emission at Mammoth Mountain, California, *Earth Planet. Sci. Lett., 188*, 535-541, 2001.

Rosi, M. and R. Santacroce, Volcanic hazard assessment in the Phlegraean Fields: A contribution based on stratigraphic and historical data, *Bull. Volcanol., 47*, 359-370, 1984.

Rosi, M. and A. Sbrana, *Phlegraean Fields: (CNR Quaderni de "La Ricerca Scientifica" 9)*, 175 pp., Conz. Naz. Delle Ric., Rome, Italy, 1987.

Savage, D., P.R. Maul, S. Benbow, and R.C. Walke, A generic FEP database for the assessment of long-term performance and safety of the geological storage of CO_2, *Quintessa Report QRS-1060A-1*, 2004.

Schminke, H.-U., P.V.D. Boogaard, A. Freundt, and C. Park, Evolution of complex Plinian eruptions: the late Quaternary Laacher See case history compared with the Minoan eruption, *Abstr. Third Int. Thera Congress, Santorini*, 1989.

Shipton, Z.K., J.P. Evans, B. Dockrill, J. Heath, A. Williams, D. Kirchner, and P.T. Kolesar, Natural leaking CO_2-charged systems as analogues for failed geologic sequestration reservoirs, In: S.J. Baines and R.H. Worden (Eds.), *Geological Storage of Carbon Dioxide*, Geological Society, London,Special Publications, 233, 43-58, 2004.

Sigurdsson, H., J.D. Devine, F.M. Tchoua, T.S. Presser, M.K.W. Pringle, and W.C. Evans, Origin of the lethal gas burst from Lake Monoun, Cameroun, *J. Volcanol. Geotherm. Res., 31*, 1-16, 1987.

Smithsonian Institution (SI), Global Volcanism Program, 1990. http://www.volcano.si.edu/gvp/index.htm

Sorey, M.L. G.A. Suemnicht, N.C. Sturchio, G.A. Nordquist, New evidence on the hydrothermal system in Long Valley caldera, California, from wells, fluid sampling, electrical geophysics, and age determinations of hot-spring deposits, *J. Volcanol. Geotherm. Res., 48*, 229-263, 1991.

Sorey, M.L., B.M. Kennedy, W.C. Evans, C.D. Farrar, and G.A. Suemnicht, Helium isotope and gas discharge variations associated with crustal unrest in Long Valley caldera, California, 1989-1992, *J. Geophys. Res., 98*, 15,871-15,889, 1993.

Sorey, M.L., W.C. Evans, B.M. Kennedy, C.D. Farrar, L.J. Hainsworth, B. Hausback, Carbon dioxide and helium emissions from a reservoir of magmatic gas beneath Mammoth Mountain, California, *J. Geophys. Res., 103*, 15,303-15,323, 1998.

Stevens, S.H., C.E. Fox, L.S. Melzer, McElmo Dome and St. John's natural CO_2 deposits: Analogues for geologic sequestration, *GHGT5*, Victoria, Australia, 2001a.

Stevens, S.H., J.M. Pearce, A.A.J. Rigg, Natural analogues for geologic storage of CO_2: An integrated global research program, *First National Conference on Carbon Sequestration*, Washington, D.C., May 15-17, 2001b

Suda, T., M. Fujii, and K. Yoshida, Development of flue gas carbon dioxide recovery technology, *First International Conference on Carbon Dioxide Removal*, Amsterdam, Netherlands, 1992.

Tedesco, D., Chemical and isotopic gas emissions at Campi Flegrei: Evidence for an aborted period of unrest, J. Geophys. Res., 99, 15,623-15,631, 1994.

Tedesco, D. and P. Scarsi, Chemical (He, H_2, CH_4, Ne, Ar, N_2) and isotopic (He, Ne, Ar, C) variations at the Solfatara crater (southern Italy): mixing of different sources in relation to seismic activity, *Earth Planet. Sci. Lett., 171*, 465-480, 1999.

Tietze, K., Cause and mechanism of the disasterous gas burst from Lake Nyos, (Cameroon/1986), Bundesanstalt für Geowissenschaften und Rohstoff, Hannover, Germany, 1987.

Tóth, E., F. Deak, C.S. Gyurkócza, Z.S. Kasztovszky, R. Kuczi, G. Marx, B. Nagy, S. Oberstedt, L. Sajó-Bohus, C.S. Sükösd, G. Toth, and N. Vajda, Radon variations in a Hungarian village, *Env. Geology, 31*, 123-127, 1997.

Varekamp, J.C., Geology and petrology of the vulsinian volcanic area (Latium, Italy), *Geol. Ultraiectina, 22*, 1-384, 1979.

Voltaggio, M. and M. Barbieri, Geochronology, In: R. Triglia (Ed.), *The volcano of the Alban Hills, Rome*, 167-192, 1995.

Waldhauser, F. and W.L. Ellsworth, A double-difference hypocenter algorithm: method and application to the northern Hayward fault, California, *J. Geophys. Res., 107*, 2054, 2000.

Watney, W.L., A.P. Byrnes, S. Bhattacharya, S.E. Nissen, and A.K. Anderson, Natural gas explosions in Hutchinson, Kansas: geologic factors, Geological Society of America, North-Central Section – 37th Annual Meeting, March 24-25, 2003.

APPENDIX A

Table A.1. Detailed summary of natural (N) and industrial (I) large releases of CO_2.

Site	Geographic setting/land use	CO_2 Source	Geologic model for accumulation	Event triggering leakage	Pathway for leakage	Type of release	Magnitude of CO_2 release	Consequences of release	Monitoring and remedial measures
N.1. Mammoth Mountain, CA USA	Recreational area (U.S. national forest, ski resort)	Magmatic + thermal decomposition of carbonates	Accumulation at ~2 km depth in porous/fractured rock under caprock	Seismic activity and reservoir pressurization	Faults and fractures	Fast, diffuse, vent, spring	~250 t d^{-1} from 480,000 m^2 area	Formation of tree kill areas, one person with symptoms of asphyxiation, one person died	Temporal and spatial monitoring of CO_2 concentrations using infrared gas analyzers and fluxes using accumulation chamber method in tree kill areas; measurements of groundwater chemistry, seismic and deformation monitoring, public education
N.2. Solfatara, Italy	Recreational area (private park/campground) surrounded by urban area	Magmatic + thermal decomposition of carbonates	Relatively shallow zone of fractured rock contains gas phase and overlies aquifers, then magma body at several km depth	No specific release event captured	Faults and fractures	Diffuse and vent	1500 t d^{-1} from 0.5 km^2 area	No vegetation in degassing area.	Temporal; and spatial monitoring of soil CO_2 fluxes using accumulation chamber and eddy covariance methods, monitoring of heat release using measurements of soil temperatures; monitoring of fumarole gas chemistry using gas chromatography; seismic and deformation monitoring; public education
N.3. Mátraderecske, Hungary	Rural area, village	Geothermal/copper -zinc mineralization	CO_2 accumulates in karst water reservoir (~1 km depth)	No specific release event captured	Faults and fractures	Diffuse, vent, spring	Average CO_2 flux ~ 200 to 400 g $m^{-2}d^{-1}$ (total degassing area unknown)	High CO_2 concentrations in homes, death of several people	CO_2 detection and control devices installed in homes, demolition of homes with hazardous CO_2 levels, public education
N.4. Latera	Rural, small towns	Thermal decomposition of	CO_2 accumulates in liquid-dominated,	No specific release event	Faults and	Diffuse, vent,	Na	Vegetation stress	Soil gas concentration

Site	Geographic setting/land use	CO_2 Source	Geologic model for accumulation	Event triggering leakage	Pathway for leakage	Type of release	Magnitude of CO_2 release	Consequences of release	Monitoring and remedial measures
caldera, Italy		carbonates, magmatic component	carbonate geothermal reservoir capped by hydrothermally altered volcanics	captured	fractures	spring		or kill	surveys using gas chromatography, hazard mapping
N.5. Albani Hills, Italy	Urban area	Magmatic + thermal decomposition of carbonates	Deep pressurized reservoirs in structural highs of sedimentary bedrock	Slow releases, with several sudden large releases also occurring, possibly triggered by seismic activity	Faults and fractures	1995 and 1999 events Fast, diffuse, vent, and spring/ well	74 t d^{-1} as surface gas emissions (61,000 m^2 area) and 506 t d^{-1} as dissolved CO_2 in shallow ground water	High CO_2 concentrations in homes; deaths of livestock (1999 event); past human deaths	Measurements of soil CO_2 fluxes and concentrations, identification of residential areas at risk, development of zoning bylaws, and development of public education programs
N.6. Dieng, Indonesia	Rural	Magmatic	Unknown	Volcanic, possibly "pneumatic", eruptions	Fissure	Eruptive	Unknown	~145 people killed	Na
N.7. Rabaul, Papua New Guinea	Rural	Magmatic	Unknown	Unknown	Fractures	Fast, vent	Unknown	Three people killed, birds killed	Na
N.8. Lakes Monoun and Nyos, Camaroon	Rural, villages	Magmatic	Accumulation in deep lake and stable stratification	Rapid lake turnover triggered at Monoun by landslide; Nyos trigger unknown	NA	Eruptive (limnic)	Nyos: 240,000 t CO_2 in eruptive event	Loss of human (~1800 combined) and animal life (e.g., thousands of cattle), plant damage	Controlled lake degassing using pipes, monitoring of lake chemistry, public education
N.9. Laacher See, Germany	Rural	Magmatic	Na	Seasonal lake overturn and mixing	NA	Diffusive and bubbling from lake surface, diffusive from lake shore	~14 t d^{-1}	Na	Measurements of CO_2 fluxes from lake surface and shore
N.10. Clear Lake, CA, USA	Rural	Thermal decomposition of metasedimentary rocks, minor magmatic component	CO_2 derived from liquid-dominated geothermal reservoir hosted in marine metasedimentary rocks	No specific release event captured	Faults and fractures	Gas vents, springs	~ 1 t d^{-1}	Four people killed	Measurements of soil CO_2 fluxes and concentrations using accumulation chamber and gas chromatography, mineral pool

Site	Geographic setting/land use	CO_2 Source	Geologic model for accumulation	Event triggering leakage	Pathway for leakage	Type of release	Magnitude of CO_2 release	Consequences of release	Monitoring and remedial measures
									closed
N.11. Paradox Basin, UT, USA	Rural	Thermal decomposition of carbonates	Reservoirs are vertically stacked, sandstone units, in fault-bounded anticlinal folds. Shale/siltstone units provide caps.	No specific release event captured	Faults and fractures	Diffuse, gas seeps, springs	Soil CO_2 fluxes up to 100 g $m^{-2}d^{-1}$; total emission rate unknown	Na	Measurements of soil CO_2 fluxes using accumulation chamber; monitoring groundwater chemistry
N.12. Florina Basin, Greece	Rural, villages	Thermal decomposition of carbonates	Reservoirs are vertically stacked, limestone and sandstone units (upper unit at 300 m depth). Capping units are silts and clays.	No specific release event captured	Slow leakage along rock discontinuities	Springs, gas seeps	Unknown	Na	Measurements of groundwater chemistry
I.1. Sheep Mountain, CO, USA	Rural	Thermal decomposition of carbonates	Reservoir is anticlinal fold, bounded on one side by thrust fault, sandstone, ave. depth 1500 m. Capped by marine sediments and a laccolith.	Well blowout	Well	Free flowing CO_2 gas from well, CO_2 leakage from fractures above drill site	Unknown	Na	Dynamic injection of drag-reduced brine followed by mud
I.2. Crystal and Tenmile Geysers, Paradox Basin, UT, USA	Rural	Thermal decomposition of carbonates	Reservoirs are vertically stacked, sandstone units, in fault-bounded anticlinal folds. Shale/siltstone units provide caps.	Well blowouts	Wells	Cold geysers	Crystal Geyser: ~33 t d^{-1}	Na	Measurements of atmospheric CO_2 concentrations using gas analyzers
I.3. Florina Basin, Greece	Rural, small towns	Thermal decomposition of carbonates	Reservoirs are vertically stacked, limestone and sandstone units (upper unit at 300 m depth). Capping units are silts and clays.	Well blowout	Well	CO_2 gas leakage from soils, water-filled pool formation around well	Unknown	Death of one person	Leakage area closed off to people
I.4. Torre Alfina geothermal field, Italy	Rural	Geothermal	Geothermal reservoir with a gas CO_2 cap at ~660 m depth. Capping units are sequences of shales, marls, and limestones.	Well blowout	Well	Free flowing CO_2 gas from well, diffuse emissions from ground around	~25,000 t	Na	Cementation of exploration well, borehole installation to focus subsurface gas flow and vent CO_2 at height in atmosphere, atmospheric CO_2

Site	Geographic setting/land use	CO_2 Source	Geologic model for accumulation	Event triggering leakage	Pathway for leakage	Type of release	Magnitude of CO_2 release	Consequences of release	Monitoring and remedial measures
						well			concentration monitoring using gas analyzers